Missouri S&T Library and Learning Resources

Scholars' Mine

Masters Theses

Student Theses and Dissertations

Spring 2014

Evaluation of ceramic coaxial cable sensors for long-term in-situ monitoring of geologic CO_2 injection and storage

Yurong Li

Follow this and additional works at: https://scholarsmine.mst.edu/masters_theses

 Part of the Petroleum Engineering Commons

Department:

Recommended Citation

Li, Yurong, "Evaluation of ceramic coaxial cable sensors for long-term in-situ monitoring of geologic CO_2 injection and storage" (2014). *Masters Theses*. 7243.
https://scholarsmine.mst.edu/masters_theses/7243

This thesis is brought to you by Scholars' Mine, a service of the Missouri S&T Library and Learning Resources. This work is protected by U. S. Copyright Law. Unauthorized use including reproduction for redistribution requires the permission of the copyright holder. For more information, please contact scholarsmine@mst.edu.

EVALUATION OF CERAMIC COAXIAL CABLE SENSORS FOR LONG-TERM IN-SITU MONITORING OF GEOLOGIC CO_2 INJECTION AND STORAGE

by

YURONG LI

A THESIS

Presented to the Faculty of the Graduate School of the

MISSOURI UNIVERSITY OF SCIENCE AND TECHNOLOGY

In Partial Fulfillment of the Requirements for the Degree

MASTER OF SCIENCE IN PETROLEUM ENGINEERING

2014

Approved by

Dr. Runar Nygaard, Advisor
Dr. Ralph E. Flori
Dr. Baojun Bai

© 2014
YURONG LI
All Rights Reserved

ABSTRACT

Monitoring is an essential component of CO_2 injection and storage projects in order to manage the injection process, identify leakage risks, provide early failure warnings, determine the movement of CO_2 plume and provide input into reservoir models. In-situ monitoring provides critical and direct data points that can be used to fulfill the above objectives. However, downhole sensors that can withstand the harsh conditions and run over decades of the project life cycle remain unavailable. A new idea of ceramic coaxial cable temperature, pressure and strain sensor has recently been put forward and the sensors are under development.

A high pressure high temperature (HPHT) testing system was developed in order to characterize the novel ceramic coaxial cable sensors under combined temperature, pressure and strain conditions with water, oil, brine, CO_2 and CO_2/brine mixture. Tests were conducted on a semi-rigid coaxial cable temperature sensor under combined temperature and pressure conditions with water. Besides, a preliminary test was conducted on the ceramic coaxial cable pressure sensor model to help with the design of the sensor.

The semi-rigid coaxial cable temperature sensor showed an excellent ability of recording the actual temperature of hydraulic water with a constant resolution of ±1℃. The preliminary test on ceramic coaxial cable pressure sensor model decided stainless steel as the proper material for sensor jacket.

ACKNOWLEDGMENTS

I would like to express my deepest gratitude to my advisor Dr. Nygaard for the great deal of patience and instruction he had for me during the past two years. He always treated me with an open mind and he is not only an academic mentor but also a friend in life. What I have learned from him is not just the passion and skills in research, but also, a positive attitude towards life and how to enjoy what I am doing all the way.

I am grateful to Michael Bassett, a talented technician from the Rock Mechanics & Explosives Research Center, without whom I would never have finished the equipment for my research. I also appreciate the valuable suggestions and feedback from the committee members Dr. Flori and Dr. Bai. I also want to thank those lovely friends in my research group, who have always been so helpful and adorable that they made each day of working together an unforgettable memory. In addition, I appreciate the financial support from US Department of Energy. This material is based upon work supported by the Department of Energy under Award Number DE-FE0009843.

Finally, my heartfelt appreciation goes to my parents, who always love me, believe me, and give me whatever they have under no conditions. And, I know they have been through a lot of challenging times spiritually in order to support me in pursuing my dreams and getting the life I want. Without their support, I would not be who I am and would not be able to achieve what I have accomplished so far. I felt sorry for the times when I was not with them and let them suffer from loneliness. I will always appreciate their unconditional love and make every effort to protect them from pain and sorrow.

DISCLAIMER

This report was prepared as an account of work sponsored by an agency of the United States Government. Neither the United States Government nor any agency thereof, nor any of their employees, makes any warranty, express or implied, or assumes any legal liability or responsibility for the accuracy, completeness, or usefulness of any information, apparatus, product, or process disclosed, or represents that its use would not infringe privately owned rights. Reference herein to any specific commercial product, process, or service by trade name, trademark, manufacturer, or otherwise does not necessarily constitute or imply its endorsement, recommendation, or favoring by the United States Government or any agency thereof. The views and opinions of authors expressed herein do not necessarily state or reflect those of the United States Government or any agency thereof.

TABLE OF CONTENTS

LIST OF ILLUSTRATIONS

Page

LIST OF TABLES

Page

LIST OF ABBREVIATIONS

Abbreviation	Description
CCBG	Coaxial Cable Bragg Grating
CCCBG	Ceramic Coaxial Cable Bragg Grating
CCCFPI	Ceramic Coaxial Cable Fabry-Perot Interferometers
CCFPI	Coaxial Cable Fabry-Perot Interferometers
CCS	Carbon Capture and Sequestration
CO_2	Carbon Dioxide
DTS	Distributed Temperature Sensing
EM	Electromagnetic
EPA	Environmental Protection Agency
ESP	Electric Submersible Pump
F.S.	Full Scale
FFPI	Fiber Fabry-Perot Interferometer
GCS	Geological Carbon Sequestration
H_2	Hydrogen
HPHT	High Pressure High Temperature
LVDT	Linear Variable Differential Transformer
OFS	Optical Fiber Sensor
OH	Hydroxyl
R.O.	Reduced Offset
RF	Radio Frequency
RST	Reservoir Saturation Tool

RTD	Resistance Temperature Detector
SNR	Signal-to-Noise Ratio
VNA	Vector Network Analyzer
WAG	Water Alternating Gas
WASP	Wabamun Area CO_2 Sequestration Project

1. INTRODUCTION

1.1. OVERVIEW

Carbon sequestration is the long-term isolation of carbon dioxide from the atmosphere through physical, chemical, biological, or engineered processes (Katzer et al. 2007). Injecting CO_2 into saline aquifers, deep coal seams, depleted gas reservoirs and several other potential reservoirs is one of the most direct methods for preventing its escape into the atmosphere, and depleted oil reservoirs are especially attractive because of their site-characterization, infrastructural and economic advantages (Bachu 2003; Pawar et al. 2004; Benson & Cole 2008).

1.1.1. Development of CO_2 Sequestration Projects. Since the start of the first carbon dioxide geological storage project in 1996 at Sleipner of Norway (Korbol & Kaddour 1995), the governments and industry around the world have been focusing more and more attention on the large scale implementation of CO_2 capture and storage, and the success of the three world's largest CO_2 storage projects have provided us with abundant experience and confidence in long-term CO_2 storage in appropriately selected geological storage sites. According to the Global CCS Institute, by February 25th 2014 there are totally twenty-one active large-scale integrated CCS projects (at least 800,000 tonnes of CO_2 annually for a coal-based power plant, or at least 400,000 tonnes of CO_2 annually for other emission-intensive industrial facilities, including natural gas-based power generation) distributed around the world, and thirty-eight planned projects in different stages of preparation (Global CCS Institute 2014).

1.1.2. Leakage Risks and its Environmental Influence. Leakage is one of the major concerns on geological carbon sequestration in addition to gravity override and possible viscous fingering due to the density difference between CO_2 and resident formation water (Nordbotten et al. 2004). Generally speaking, leakage of geologically stored CO_2 can occur in several different ways as shown in Figure 1.1 (Nygaard et al. 2013). Four main types exist: (1) through matrix (such as high permeability zones), (2) through pathways (such as faults, fractures), (3) through geomechanics (such as hydraulic fractures, earthquakes) and (4) through wellbores. The main leakage risk of CO_2 through a thick, low permeable cap rock is identified to be along existing wells or through faults and fractures.

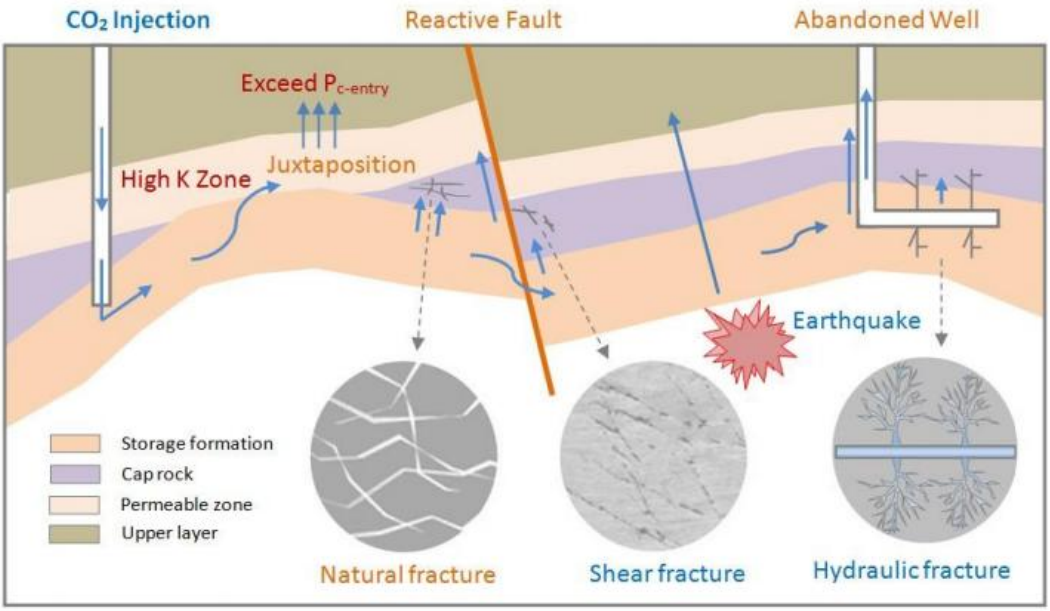

Figure 1.1 Possible CO_2 Leakage Mechanisms in Reservoir.

Injection takes place in sedimentary basins that often have a history of oil and gas exploration and production, which means that wells other than those used for waste disposal may exist in the vicinity of the injection site. These existing wells provide possible pathways for leakage of waste fluids toward the shallow subsurface and the land surface (Nordbotten et al. 2004). The cement sheath is one of the primary barriers to prevent wellbore leakage and failure. The integrity of the cement sheath begins at the cementing operation and what happens there can greatly affect the long term integrity of the well (Weideman & Nygaard 2014). The various leakage paths that can occur in the near wellbore region are presented in Figure 1.2.

The benefits of sequestration would be negated if leakage occurs. Adverse health, safety, and environmental consequences may be caused by accumulated high concentration CO_2 if it is leaked into a contained environment. The safety of drinking water would also be taken into account in the case of injecting fluid into subsurface. Chemical detection of leakage into shallow aquifers from a deep CO_2 geo-sequestration site will be an integral part of a safe CCS system. CO_2 that infiltrates an unconfined freshwater aquifer under oxidizing conditions and atmospheric pressure will have an immediate impact on water chemistry by lowering pH and increasing the concentration of total dissolved solids (Little et al. 2010).

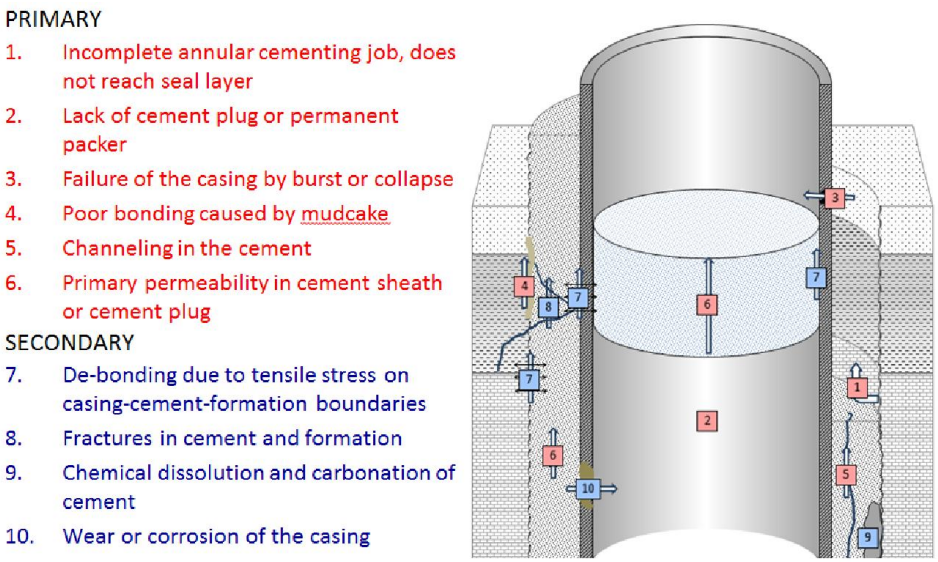

Figure 1.2 Leakage Paths in Near Wellbore Region.

1.1.3. Challenges on Prediction of CO_2 Plume and Leakage Detection. Tremendous challenges are imposed to determine the transport and predict the fate of stored CO_2 due to the inaccessibility and complexity of the potential storage formation and the sealing formations in the subsurface, the wide range of scales of variability, and the coupled nonlinear processes (Martens et al. 2012). Comprehensive models of fluid flow in porous media are used to simulate the CO_2 flume evolution and evaluate the transient flow rate through the artificial conduits and the resulting hydraulic head distributions (Avci 1994; Huang et al. 2014; Nordbotten et al. 2004, 2005; Zeidouni 2014). However, the validation of such models is very challenging due to the limited understanding and inadequate data available for characterization of the subsurface temporal and spatial state variables and geologic media properties.

1.1.4. Challenges on Monitoring Technologies. A program for monitoring of CO_2 distribution is required once injection begins in order to manage the injection process, delineate and identify leakage risk or actual leakage that may endanger underground source of drinking water, verify and provide input into reservoir models, and provide early warnings of failure. Monitoring of the wells, deep subsurface, shallow subsurface and ground surface is expected to continue for long periods after the injection is terminated for safety and to confirm predictions of storage behavior (United States Environmental Protection Agency 2008).

To ensure the public safety as well as obtaining carbon credits in a future cap and trade system, monitoring and modeling of sequestration projects have to reach a high degree of accuracy. The objective is to reach 99% accuracy in a monitoring and verification program (The National Energy Technology Laboratory 2009). However, the predictions based on current methodology are far too uncertain to achieve the goal to account for 99% of the injected CO_2 (The National Energy Technology Laboratory 2012).

Among the various monitoring approaches, in situ downhole monitoring of state parameters (e.g., pressure, temperature, etc.) provides critical and direct data points that can be used to validate the models, optimize the injection scheme, detect leakage and track the CO_2 plume (European Commission 2013; Freifeld 2009; United States Environmental Protection Agency 2008; Benson et al. 2004). However, the downhole monitoring usually deals with high pressure high temperature (HPHT) conditions (T ≥175℃, P ≥15,000 psia), ultra HPHT conditions (T ≥200℃, P ≥20,000 psia), or even extreme HPHT conditions (T ≥250℃, P ≥30,000 psia) (Castro 2013). Downhole sensors that can withstand the harsh conditions and operate over decades of the project lifecycle remain unavailable.

Given that the widespread of carbon capture and storage will be the necessity and reality in the future, fundamental and applied research is required to address the significant challenges and technological gaps in developing reliable long-term sensors that can operate in downhole environments.

1.2. CURRENT MONITORING TECHNOLOGIES RELEVANT TO CO_2 SEQUESTRATION

Various sensing technologies have been explored for characterization and monitoring of subsurface geologic environments. The current monitoring technologies relevant to CO_2 sequestration can be classified into four categories, which are repository-based monitoring, well-based monitoring, surface-based monitoring and remote monitoring (European Commission 2013). A comprehensive summary focused mainly on well-based monitoring technologies and fiber optic sensor as a progressively developed repository-based monitoring technology is provided below.

1.2.1. Well-Based Monitoring. Recent CO_2 sequestration pilot projects have implemented novel approaches to well-based subsurface monitoring aimed at increasing the amount and quality of information available from boreholes. Well

based-monitoring of oil and gas reservoirs includes a broad array of techniques, using a diverse suite of instruments. During drilling, core is often recovered to permit petro-physical measurements and provide fluid saturation information. Core plugs from the larger core are often extracted to measure permeability and porosity and segments of core can be used to conduct core fluid studies. Wireline logs provide information using non-contact methods (e.g. neutrons, seismic and electrical waves) to periodically interrogate the formation. In addition, permanently deployed sensors and repeat geophysical surveys can assess changes in the subsurface (Freifeld et al. 2009).

1.2.1.1 Wireline logging. Wireline logging includes a wide variety of measurement techniques in which a sonde is trolled through a wellbore and data is transmitted from sensors to surface for recording. Commonly used wireline logs include gamma ray density, formation resistivity, acoustic velocity, self-potential, temperature and pressure. New and more sophisticated tools including formation microimagers, neutron cross-section capture, and nuclear magnetic resonance scanners have been developed by the oilfield service providers. Besides, there are wireline tools to collect fluid samples (e.g. the Kuster flow through sampler) and retrieve sidewall cores for later analysis (Freifeld et al. 2009).

The Frio Brine Pilot Test conducted in 2004 consisted of the injection of 1600 tons of CO_2 in a steeply dipping brine saturated sandstone beneath a shale caprock (Hovorka et al. 2006). The Schlumberger wire-line reservoir saturation tool (RST) used pulsed neutron capture to determine changing brine saturation as brine was displaced by CO_2. Sigma ($\sum$), the parameter collected by the RST tool, is derived from the rate of capture of thermal neutrons (mainly chlorine). The high value of $\sum$ for formation water derived from brine conductivity allows estimation of water saturation and the inverse, CO_2 saturation (Sakurai et al. 2005). Corrections were made for borehole conditions due to the change of fluids and completions to accommodate other instrumentation. The results of wire-line logs show the changing conditions within and immediately outside the wellbore at fine vertical resolution. The interpreted saturation from RST suggests that, as predicted, evaporation of residual water into dry CO_2 occurred near the injection wellbore. However, considering the open borehole along the perforated zone, the well-based measurement in predicting CO_2 saturation in deeper formation is not representative.

1.2.1.2 Geophysical techniques. Near field geophysical technique requires only a single borehole and can be performed at any depth range, and sense the properties of the borehole itself and its immediate vicinity. These is a wide variety of techniques with regard to geophysical monitoring, e.g., borehole televiewer (optical), caliper logs, resistivity logs, electromagnetic induction logs, Gamma logs (passive and active), Neutron logs, sonic logs etc. These techniques can determine the near-borehole structures with a high accuracy. Far field geophysical techniques provide information up to greater distances. This technique includes single-hole and cross-hole geoelectric tomography, georadar and seismic methods. The far-field methods have the potential of characterizing anomalous features at quite some distances away from a borehole, but all of them are faced with an inherent limitation.

Surface and surface-downhole seismic measurements were applied in the CO_2 storage project at Ketzin, Germany (Martens et al. 2012). The time-lapse 3D surveys were carried out in 2005 (baseline) and 2009 (first repeat). The CO_2 signature could be detected by an increase reflectivity at the top of the target reservoir, by a change in the attenuation behavior and by a reduced propagation velocity within the reservoir (Lüth et al. 2011). The quantitative analysis of the CO_2 contained in the area of the seismic time-lapse amplitude anomaly showed that the mass distribution of the imaged CO_2 can be compared to the history-matched reservoir simulations. It indicates a general consistency of the simulation with the monitoring results and qualitatively shows the existence of a detection threshold for the seismic monitoring which is not imaging the more distant parts of the CO_2 plume away from the injection point. However, some limitations of using seismic surveys to monitor CO_2 sequestration have been identified (Cairns et al. 2010). The smallest detectable amount of CO_2 depends on the fluid distribution, if homogeneously distributed, 1% CO_2 is detectable, however if patchily distributed anything below 18% CO_2 is indistinguishable from brine.

In part due to the success at Sleipner, 4-D seismic has emerged as the standard for comparison (Chadwick et al. 2004). This technology shows great advantage at delineating the boundaries of a free-phase CO_2 plume, and can detect small saturations of conjoined free-phase bubbles that might be an indicator of leakage. Results from these 4D-seismic surveys are part of the grounds for belief in the long-term effectiveness of geological sequestration.

1.2.1.3 Geochemical sampling. Geochemical sampling is used to assess rock-water interaction in order to better understand the ultimate fate of emplaced CO_2 and assess the integrity of reservoir seals. Abundant amount of methods have been devised to obtain representative downhole samples while maintaining reservoir pressure conditions. Downhole fluid samples can be collected for surface analysis using wireline formation testers (e.g. the Schlumberger Modular Formation Dynamics Tester) and U-Tubes technology which is developed for the DOE Frio Brine project (United States Environmental Protection Agency 2008).

In the CO_2 storage project at Ketzin, Germany, a comprehensive surface monitoring network has been established at the Ketzin pilot site since 2005 in order to identify and monitor upward migration of CO_2 with potential leakage to the surface (Martens et al. 2012). This network consists of 20 sampling locations for soil CO_2 gas flux, soil moisture, and temperature measurements distributed across a study area of approximately 2 km × 2 km (Zimmer et al. 2011). In March 2011, the surface monitoring network was expanded by the installation of eight permanent stations with automated soil gas samplers in direct vicinity of the injection and monitoring wells. At these eight locations, CO_2 gas flux, soil moisture and temperature are measured on an hourly basis. Since the start of injection in 2008, no change in soil CO_2 gas flux could be detected in comparison to the preinjection baseline (2005–2007).

1.2.1.4 Integrated well-based monitoring. In integrated well-based monitoring, each tool is sequentially deployed in the wellbore for one purpose, and is later retrieved so that a second activity or operation could be conducted. While the risks are often low for carrying out each data collection effort since they rely on off-the-shelf products, there is considerable cost in each mobilization into and out of a well. Furthermore, data is “lost” as each tool is removed to permit access for the next tool. Several CO_2 demonstration projects have taken an integrated monitoring approach, where several measurements cutting across different disciplines are conducted simultaneously using one completion. Three programs that have taken this integrated approach are the Frio Brine Pilot and CO2SINK project, both conducted in a saline reservoir, and the Otway project, consisting of an injection in a depleted gas reservoir (Freifeld 2009).

1.2.2. Fiber Optic Sensors. Optical fiber sensors (OFS) are able to perform efficient monitoring with their multiplexing ability and reduced size compared with other wire-connected downhole sensors (United States Environmental Protection

Agency 2013). Fiber optic based downhole temperature, pressure and strain sensors for petroleum industry application are currently available (Tardy et al. 2011; Koelman et al. 2011; Costello et al. 2012; Medina et al. 2012; Molenaar et al. 2012). One configuration of fiber optic downhole monitoring is based on multiplexing discrete sensors such as high temperature fiber Bragg gratings (FBG) and Fabry-Perot interferometers (FPI) (Schmidt-Hattenberger et al. 2004; Pan et al. 2010). These microsensors passively and linearly transduce the temperature/pressure to optical signals that are transmitted to the interrogation instrumentation on the surface at a speed of light (Lee 2003). The other popular configuration of fiber optic downhole monitoring is using time-domain technique to realize truly distributed sensing. Continuous temperature profile along the entire length of an optical fiber can be mapped with decent accuracy by several mechanisms including Rayleigh scattering, Raman scattering and Brillouin scattering (Tardy et al. 2012; Molennar et al. 2012; Williams et al. 2000).

1.2.2.1 Fiber optic sensing technology under application or development. Various fiber optic downhole sensing technologies are currently at different stages of development. Distributed Temperature Sensing (DTS) is the most mature technology, with a history of successful downhole applications dates back to 18 years ago (Karaman et al. 1996). Occidental installed DTS systems in 5 of their wells on the Cogdell field during 2003 to monitor both the injection and production from the reservoir and to identify the reservoir layers that were receiving pressure support and producing as a result of the WAG flood in this complex carbonate reef reservoir (Brown et al. 2004). The optical fiber was installed in 1⁄4 inch control line outside of the production tubing (only connected to the tubing at clamp points) and supported across the reservoir interval by a stinger hung below the Electric Submersible Pump (ESP). DTS temperatures from all 5 wells have been continuously recorded since May 2003 using a single DTS laser system acquiring data in sequence from each well. Temperature profile is acquired every meter along the length of the optical fiber and the profile can be interpreted to give information about the injection and production profiles in the well. The temperature response over the reservoir at up-dip producer #1 confirms that this upper interval is the zone producing the oil and CO_2.

A Distributed Strain Sensing (DSS) technology under the name of SureView RTCM^{TM} (Real Time Compaction Monitoring) system was developed by Shell and Baker-Hughes in 2003 and successfully deployed in Shell's Pinedale operations in

Wyoming during 2008 on 7-in casing (Baker Hughes Incorporated 2010a, 2010b). The SureView monitoring, alongside the DTS and pressure gauge measurement, showed for the first time ever, behind casing, strain pressure and temperature data throughout the entire cement pumping and curing process.

Other distributed fiber optic sensing technologies such as Distributed Acoustic Sensing (DAS), Distributed Chemical Sensing (DCS) and Distributed Pressure Sensing (DPS) are still under development or in the stage of field testing (Molenaar et al. 2011, 2012; Koelman 2011; Choi et al. 2011).

1.2.2.2 Limitations of fiber optic sensors. Despite its significant advantages and progressively increasing application for downhole monitoring in oil industry, optical fiber sensors do have some inherent drawbacks that have to be evaluated when they are considered as an alternative to conventional electronic transducers. Attenuation and longevity of the system would be a major concern. Hydrogen (H_2) attenuation, liquid ingress and micro-bending effects are the three factors that will give rise to either intrinsic or extrinsic energy loss (Williams et al. 2000).

H_2 affects the fiber optic sensor either by absorption or absorption of the chemical reaction products. Absorption of H_2 that diffused into the interstitial sites in the silica network will prevent the transmission of light at required wavelength. Chemical reaction products, such as the hydroxyl (OH) groups, will absorb strongly in the transmission region of interest (1.38, 0.95 and 0.72 μm, with the strongest being at 1.38 μm). Three main methods have been developed to reduce the effect H_2 of on the optical transmission of optical fibers, such as altering the fiber dopant compositions to reduce chemically induced attenuation, redesigning the fiber cables to avoid the possibility of H_2 or H generation, and employing hermetic coatings on the fiber to block the diffusion of any H_2 that may be present, while hermetic coating is the most efficient method, particularly at elevated temperature.

Liquid ingress is another factor that has to be taken into account for design of fiber optic downhole sensing system. The ingress (i.e. entrance) of liquids into optical fibers can lead to both increases in fiber attenuation and eventual mechanical failure of the fibers. Decomposition products passing into the fibers can create absorptive losses in the waveguide and more significantly, cause mechanical damage to the fiber that leads to micro-bending effects. Water is extremely harmful to optical fibers. The presence of water, if permitted, will extend any surface cracks that may naturally occur in the fiber surface and these will be elongated by a stress cracking process. The

mechanical strength of the optical fiber will be reduced until it cannot support its own weight to cause permanent failure. Once again hermetic coating is the traditional way to mitigate the influence of water.

Micro-bending will add to increased extrinsic energy losses. Care has to be taken to avoid forming micro-bends particularly at higher temperatures in the region of 250℃. Heating and cooling of the fiber can build up stress in the coating to cause micro bending, and cyclical heating and cooling is the worst case with regard to micro bending. Tests performed for Canadian cyclic steam operations indicate that there is severe micro bending when the fiber is returned to ambient reservoir conditions after being exposed to temperatures as high as 340 °C.

1.3. COAXIAL CABLE SENSORS AS A NEW SUBSURFACE SENSING TECHNOLOGY

Although great progresses have been made in downhole sensing techniques over the last few decades to satisfy the needs of petroleum industry, the currently available sensors do not meet the needs for CO_2 sequestration monitoring. Low cost, robust, multi-agent, long-term, distributed and continuous sensing technologies that can monitor the various state parameters in deep geologic formations with high spatial and temporal resolutions are desired to determine the fate of the emplaced CO_2 and the ultimate efficacy of CO_2 storage.

1.3.1. Introduction to Coaxial Cables. Coaxial cable is a cylindrical electromagnetic (EM) waveguide consisting of an inner and an outer conductor sandwiched by a tubular insulating layer typically made of a material with a high dielectric constant. Figure 1.3 shows the comparison between coaxial cable and optical fiber cable (Tkgd2007 2008; Belkin International Incorporated 2012). Governed by the same EM theory, the two types of transmission lines share the common fundamental physics.

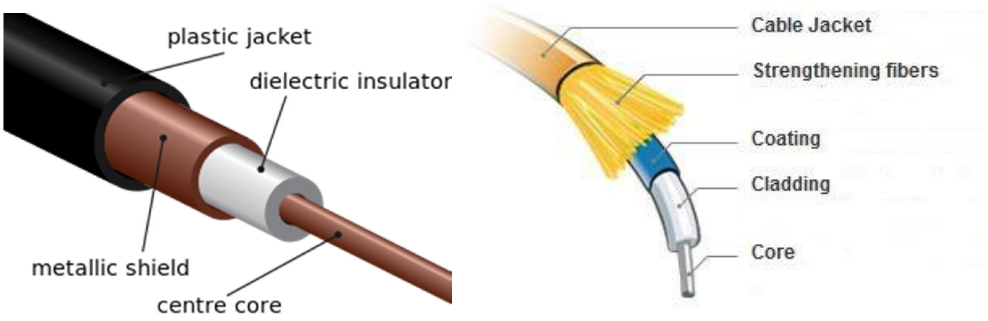

Figure 1.3 Comparison between Coaxial Cable (Left) and Optical Fiber Cable (Right).

In comparison with optical fibers, coaxial cables are much more robust and easy to be deployed. Unlike an optical fiber that has to use high quality fused silica glass, the coaxial cable operating principle allows flexible choices of materials including ceramic, silica and other high temperature tolerant dielectrics for sensor construction. The size of coaxial cables can also be varied without significant influences on signal transmissions. In addition, coaxial cables operate in radio frequency (RF) domain where the matured RF measurement technologies readily provide ample off-the-shelf components and instruments for low-cost sensor interrogation and multiplexing.

1.3.2. Coaxial Cable Bragg Grating Sensors. A novel idea of CCBG sensor was put forward inspired by the well-known fiber Bragg grating (FBG) sensor (Wei et al. 2011). A CCBG sensor was fabricated by drilling non-through holes of equal-distance into a coaxial cable (RG-58/U), which is shown in Figure 1.4. The distance between two neighboring holes was 64 mm. When interrogated using a Vector Network Analyzer (VNA), the CCBG produced transmission and reflection spectra. Bragg resonant peaks can be clearly identified with an excellent signal-to-noise ratio (SNR). The hole-drilling did not introduce observable background loss. The resonant frequency of the CCBG was found increasing almost linearly with the increase of temperature and the strain resolution can be estimated to be as high as a few με given the 1 kHz resolution in spectrum measurement of the RF VNA used in experiments.

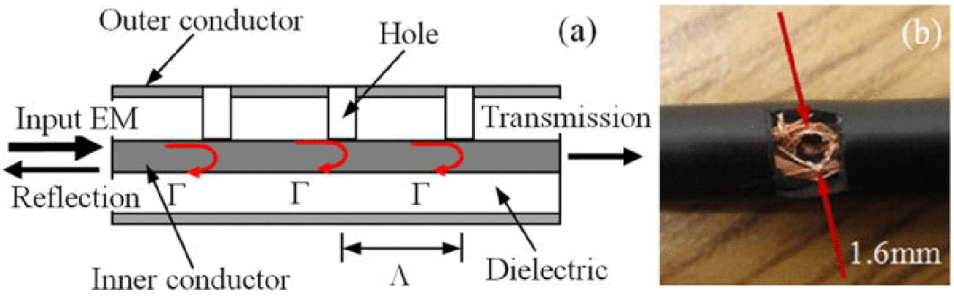

Figure 1.4 Coaxial Cable Bragg Gratings. (a) Schematics, (b) Microscopic Image of Drilled Open Hole.

1.3.3. Coaxial Cable Fabry-Perot Interferometer Sensors. Similarly, inspired by the optical fiber inline Fabry-Perot interferometer (FFPI), a CCFPI sensor was made by drilling two small holes distanced at 60 mm into the coaxial cable (RG-58) as two reflectors, which is shown in Figure 1.5 (Huang et al. 2013). The EM wave traveling inside the cable is partially reflected at the first reflector while the remaining energy transmits through to reach the second reflector. At the second reflector, the EM wave is again partially reflected. The two reflected waves travel backwards and interfere coherently to generate an interference signal. When observed in the spectrum domain, the interference signal manifests itself as an interferogram. It is exactly the same way as in the case of a FFPI. Both the temperature and strain test results showed that the resonant frequency increases almost linearly or quasi-linearly with the increasing temperature or strain. The linear temperature-frequency shift relation and quasi-linear strain-frequency shift relation indicates that CCFPI can be used as sensors for temperature and strain after it is properly calibrated.

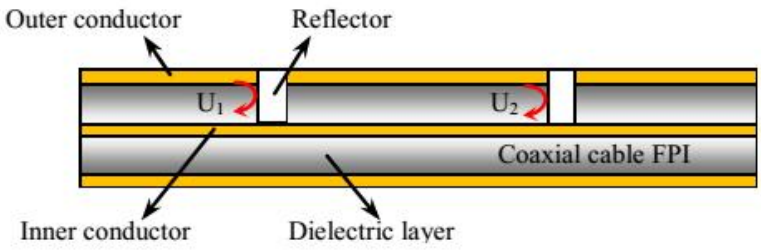

Figure 1.5 Schematic of a CCFPI.

1.3.4. Potential for Ceramic Coaxial Cable Sensors. The CCBG and CCFPI sensors made of regular coaxial cable are not suitable for the subsurface environment applications due to the high pressure and high temperature harsh downhole environment. Fortunately, the coaxial cable operating principle allows a flexible choice of materials including ceramic, silica and other high temperature tolerant dielectrics. In fact, high temperature coaxial cables are now commercially available with reasonable cost, e.g., the mineral insulated coaxial cables manufactured by Thermocoax Inc., as shown in Figure 1.6 (Thermocoax Incorporated 2012a). These cables are made by using various ceramic materials as the insulation layer so they can operate at high temperatures up to 1000℃ and high pressures up to 10,000 psia. The cables operate in the frequency range up to 20 GHz, have the necessary flexibility for deployment, and a very small attenuation of 0.08 dB/m that allows the signal to be transmitted over a long distance (Thermocoax Incorporated 2012b).

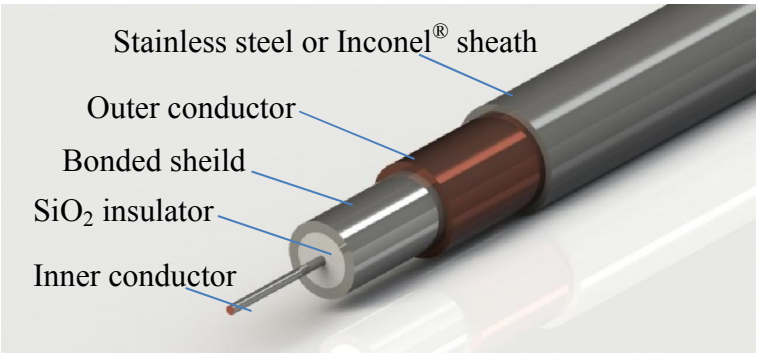

Figure 1.6 Structure of a Ceramic Coaxial Cable Manufactured by Thermocoax Inc.

It is worth noting that the CCCBG and CCCFPI sensors have their own advantages and disadvantages and they may complement each other for sensing applications. For example, the CCCBG sensor has high measurement sensitivity and can be densely multiplexed for distributed sensing. However, a CCCBG sensor is expected to have a relatively long gauge length (~0.3m) and thus a relatively low spatial resolution (but enough for the intended applications). On the other hand, CCCFPI sensor has a small gauge length (~3cm) but a high signal loss. In addition,

these two sensors can be designed to have different responses to the state parameters. As a result, mixing the two sensors in one package may achieve simultaneous measurements of multiple parameters for the purpose of temperature compensation and sensor self-calibration.

1.4. SCOPE OF WORK

The main objective of this three-year program is to conduct fundamental and applied research that will lead to the successful development and demonstration of a novel, robust, downhole ceramic coaxial cable based sensing technology for in-situ monitoring of geologic CO_2 injection and storage. Specifically, it includes: (1) develop robust ceramic coaxial cable sensors for remote measurement of temperature, pressure, and strain in a high-temperature, high-pressure downhole harsh environment; (2) develop high-performance sensor interrogation methodology and instrumentation with self-compensation capability for long-term, maintenance-free operation and dense-multiplexing capability for cost reduction; (3) integrate sensor data with the geological models for intelligent sensor deployment/installation, rational interpretation of the sensor outputs, improved accuracy of plume tracking, optimized CO_2 injection, and sensor-verified model prediction; and (4) characterize the performance and demonstrate the critical functions of the developed sensors and instrumentation for downhole applications in relevance to CO_2 sequestration monitoring.

The objective of this research is to prove the feasibility and demonstrate the performance of the new CCCBG and CCCFPI sensors for in-situ measurement of temperature, pressure and strain in downhole environments.

The first step of the research is the fabrication of the testing equipment in close simulations of actual application situations. The equipment is supposed to provide a simulated downhole environment of 300℃ and 10,000 psia and function properly with circulating water, brine, oil, CO_2, and CO_2/brine mixture.

The effectiveness of the functionality of the equipment will be tested once it is fabricated. A few sample tests will be conducted to provide information for re-design or further improvement of the equipment, and different testing methods will be compared to establish a feasible and reliable testing procedure.

Performance testing of the temperature, pressure and strain sensors will first be conducted with water after the testing procedure is established. The controlled environmental data and sensor data will be acquired to analyze the accuracy and hysteresis of the sensors. Different fluid compositions, e.g. brine, oil, CO_2, and CO_2/brine mixture, will be applied to the sensor performance tests once the test with water is proved to be effective.

Sensor long-term performance will be tested under various downhole harsh conditions. Tests will be conducted at different temperatures, pressures and fluid compositions with varying CO_2 content for a long time period. The long-term accuracy, robustness, and survivability of the sensors will be evaluated.

As a result, a sensor performance matrix under simulated downhole conditions will be generated as guide for in-situ monitoring of CO_2 injection and storage wells.

2. METHODOLOGY

2.1. SUMMARY OF STUDY

The evaluation of ceramic coaxial cable sensors includes evaluation on temperature, pressure and strain sensors. A HPHT sensor testing system will be designed and fabricated to simulate the downhole environment. Static tests under various temperature, pressure and strain conditions will be conducted on the three kinds of sensors with water, oil, brine, CO_2 and CO_2/brine mixture to establish the performance matrix of the sensors in downhole environment. Finally, tests on sensor long-term stability and survivability will be conducted by cyclic heating and cooling of the system to further evaluate their performance in simulated downhole conditions. The study can be summarized as in Figure 2.1. The parts marked with a deeper color are those that have been finished so far.

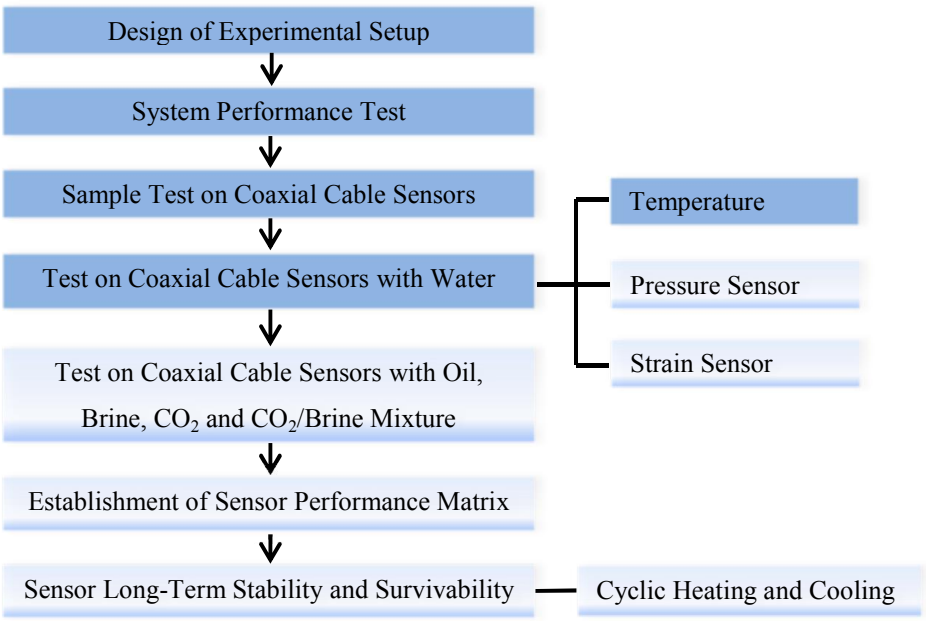

Figure 2.1 Summary of Study.

2.2. DESIGN OF EXPERIMENTAL SETUP

2.2.1. Determination of Testing Range. To test the sensor robustness under reservoir conditions a pressurized cell test up has been designed. The testing range of the three parameters (temperature, pressure and strain) is built on the field operational range, the expected sensor range and commercially available devices and fabrication techniques. The field operational range is based on the field data from several currently active large-scale integrated CO_2 sequestration projects (Wright et al. 2009) and the expected sensor range is provided by Dr. Hai Xiao and his research group from Clemson University, which is a participating team in this project. The field operational range and expected sensor range are shown in Table 2.1 and Table 2.2, respectively, and the corresponding sensor testing range is given in Table 2.3.

Table 2.1 Field Operational Range.

Parameters	Extreme Min	Min	Max	Extreme Max
Temperature (^oC)	5	27	200	250
Pressure (psia)	14.7	1450	10,000	14,000
Strain (%)	0	0.04	10	25

Table 2.2 Expected Sensor Range.

Parameters	Extreme Min	Min	Max	Extreme Max
Temperature (^oC)	0.5	2	600	800
Pressure (psia)	0	1	5000	10,000
Strain (%)	0.001	0.01	10	15

Table 2.3 Testing Range.

Parameters	Extreme Min	Min	Max	Extreme Max
Temperature (^oC)	25	30	200	230
Pressure (psia)	14.7	50	5000	10,000
Strain (%)	0	0.1	5	10

2.2.2. System Design. According to the testing range, the testing cell is required to have a pressure rating of 10,000 psia, a temperature rating of 200 ^{o}C and a strain rating of 10%. The system will be capable of handling single phase fluid circulation of water, oil, brine, CO_2, and CO_2/brine mixture. A schematic of the system design is given in Figure 2.2.

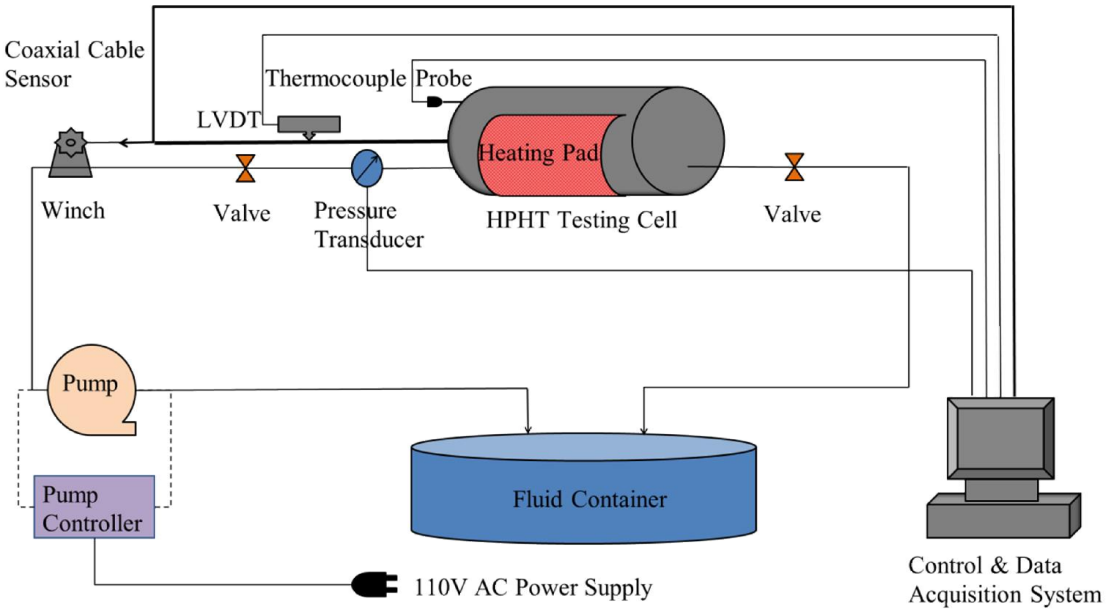

Figure 2.2 Schematic of HPHT Sensor Testing System.

2.2.3. Cell Design. To fit the sensor within the cell the cell has to have a length of 30 cm and an inner diameter of 5 cm. Heating pad and insulation material will be attached to the outer wall of cell. The heating of the fluid is governed by the temperature controller which connects to the heating pad. The schematic of cell design is shown in Figure 2.3, where 1-Thermocouple probe entrance; 2-Cable entrance; 3-Fluid entrance; 4-Cable fastener; 5-Fluid exit.

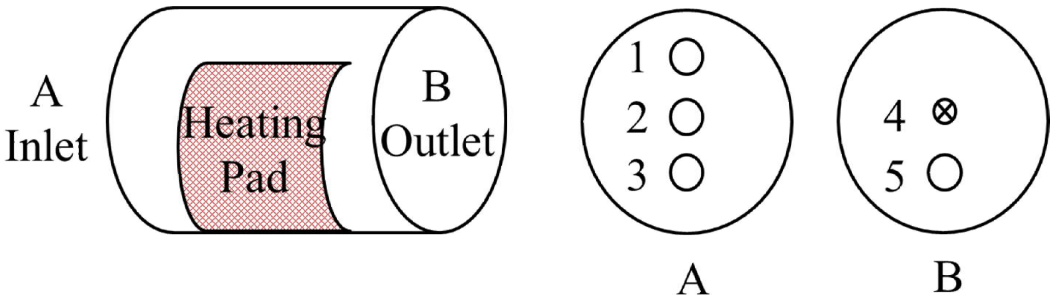

Figure 2.3 Schematic of Cell Design.

2.3. SYSTEM WORKING MECHANISM

The coaxial cable sensors are placed inside the HPHT testing cell. One end of the cable is fastened at the center of the outlet end cap and the other goes through the center of the inlet end cap then connects to a vector network analyzer which generates the RF signal and monitors the reflection spectrum.

The fluid inside the cell is heated by the heating pad at a specified rate. The insulation material will reduce the heat loss. When the heating and heat loss processes are balanced, the cell will reach a constant temperature. The actual temperature of the fluid inside the cell is measured by the thermocouple probe which goes through the entrance on the inlet end cap as shown in Figure 2.3. The temperature measurement of the coaxial cable temperature sensor will be compared with that of the thermocouple probe (serves as a standard measurement).

Pressurizing of the cell is reached by the pump. The pump should be able to maintain the cell pressure constant. The actual pressure inside the cell is measured by the pressure transducer. The measurement of pressure transducer will serve as a standard measurement. The coaxial cable pressure sensor measurement will be compared with that of the pressure transducer.

A winch is utilized to apply force to the cable. The force is measured by a force gauge connected between the winch and the cable. A test will first be conducted on the cable to find out the maximum force that the cable can endure and the force applied to the cable should always be smaller than the maximum force in all strain tests so that the cable would not be pulled apart. The displacement created on the cable will be monitored by the Linear Variable Differential Transformer (LVDT), and

the displacement will be converted into strain based on the strain-displacement correlation. The strain converted from displacement δ will serve as a standard strain and will be compared with the coaxial cable strain sensor measurement.

Since the strain on sensor under high temperature condition is caused both by thermal expansion $\delta_1$and mechanical force δ_2, the strain sensor measurement will include both of them. However, the mechanical deformation is our main interest on strain sensor under downhole environment. Thus, the strain sensor measurement needs to be calibrated. The strain sensor will first be tested under various temperature and pressure conditions without any mechanical force. The sensor measurement will be recorded and a matrix of sensor thermal expansion response under various temperature and pressure conditions will be generated. Then the strain sensor will be tested under the same temperature and pressure conditions but with a certain force, and the total strain sensor measurement will be recorded as δ_3. Suppose the sensor thermal expansion under the same temperature and pressure condition remains the same regardless of the mechanical force, then simply,

$$\delta_2 = \delta_3 - \delta_1 \qquad \text{Equation 2.1}$$

Where δ_1, δ_2 and δ_3 are obtained under the same temperature and pressure conditions. Compare the strain converted from displacement δ (standard strain measurement) with the sensor measured strain δ_2, the accuracy of the strain sensor can be acquired.

2.4. OPERATION PROCEDURES

Operation procedures of this testing system for temperature, pressure and strain tests have been established. The procedures for temperature and pressure tests obey the following.

1. Put the coaxial cable temperature (or pressure) sensor through the inlet end cap entrance into the testing cell. Fasten the cable end to the outlet end cap and seal the cell.
2. Wrap the insulation blanket around the cell.
3. Open the inlet valve and close the outlet valve. Pump water (or oil, brine, CO_2, CO_2/brine mixture) into the cell until the cell is filled with liquid or gas.

4. Set the pump pressure to constant P1. Keep recording the pressure inside the cell with the pressure transducer until it reaches constant.
5. Set the temperature controller at T1. Keep recording the temperature inside the cell with the thermocouple probe until it reaches constant.
6. After both the temperature and pressure inside the cell has reached constant, start recording the coaxial cable temperature or pressure sensor response with the VNA.
7. Increase the temperature controller to T2 or pump pressure to P2. Repeat the same procedure for the previous temperature/pressure test.
8. Take off the insulation blanket. Reduce the temperature controller to T1' or pump pressure to P1'. Repeat the same procedure for the previous temperature/pressure test.
9. Repeat tests until the cell temperature and pressure go back to the initial conditions.
10. Open cell. Discharge all the liquid or gas. Take out the coaxial cable sensors for integrity examination.

The strain test would first follow the same procedures as stated above in order to get the strain sensor response matrix under various temperature and pressure conditions. Then the following procedures need to be completed to test the strain sensor performance.

1. Put the coaxial cable strain sensor through the inlet end cap entrance into the testing cell. Fasten the cable end to the outlet end cap.
2. Apply a force F1 on the cable with the winch then seal the cell.
3. Wrap the insulation blanket around the cell.
4. Open the inlet valve and close the outlet valve. Pump water (or oil, brine, CO_2, CO_2/brine mixture) into the cell until the cell is filled with liquid or gas.
5. Repeat the same procedures as in the temperature and pressure sensor tests.
6. Release the stress on cable. Open cell. Discharge all the liquid or gas. Take out the coaxial cable sensors for integrity examination.
7. Same steps would be repeated in test under force F2.

2.5. EVALUATION OF SENSOR SHORT-TERM AND LONG-TERM PERFORMANCE

Prior to the test on coaxial cable sensors, a pretest needs to be conducted to examine the functionality and efficiency of the whole system. Items need to be checked include the maximum temperature the cell can be heated and how fast the heating speed is, how long it takes for the temperature to go down, and the maximum pressure the cell can withstand without leakage.

Water is first used as fluid environment in the cell. Tests on temperature, pressure and strain sensors would follow the operation procedures illustrated in the previous section. Later the tests will be conducted with oil, brine, CO_2 and CO_2/brine mixture. A matrix of coaxial cable sensor performance under various temperature, pressure and strain conditions will be generated.

Since the downhole application of the coaxial cable sensors would be dealing with constantly changing environments, and vibrating temperatures are believed to cause serious damage to the sensor robustness, tests will be conducted to evaluate the sensor long-term stability and survivability by cyclic heating and cooling of the cell. The sensor accuracy and integrity in the long-term test will be compared with the short-term test results.

3. RESULTS

During the past five quarters, part of the research objective has been completed as planned, including the fabrication and pretest of the HPHT sensor testing system, the characterization of coaxial cable temperature sensor under various temperature and pressure conditions with water, and the preliminary test on coaxial cable pressure sensor model.

3.1. FABRICATION AND PRETEST OF HPHT SENSOR TESTING SYSTEM

A HPHT testing cell has been fabricated and the system has been completed for sensor testing under various temperature, pressure and strain conditions based on the system schematic given in Figure 2.2. A picture of the whole system set up is shown in Figure 3.1.

Figure 3.1 Picture of the HPHT Sensor Testing System.

3.1.1. HPHT Testing Cell. A testing cell is fabricated with stainless steel as container for HPHT fluid and coaxial cable sensors. The cell has a length of 30 cm and an inner diameter of 5 cm. The end caps are fabricated as has been clarified in Figure 2.3. A picture of the cell is shown in Figure 3.2.

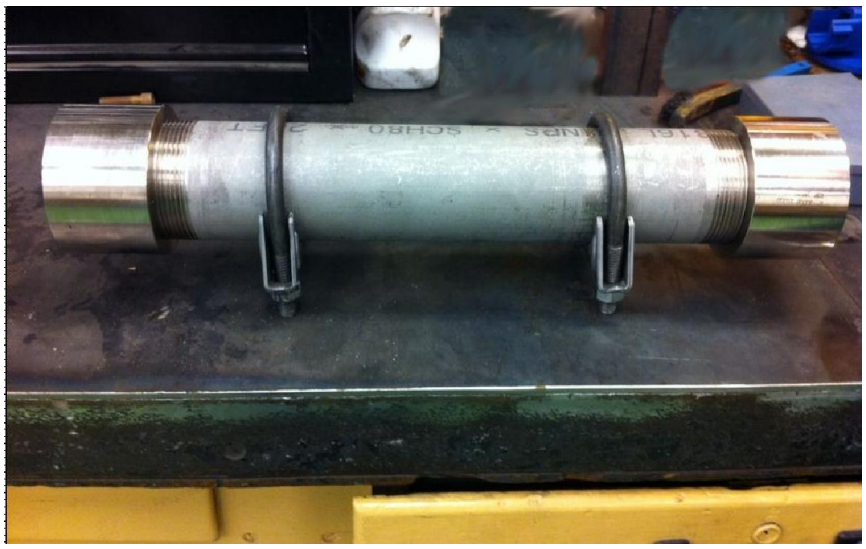

Figure 3.2 Picture of HPHT Testing Cell.

3.1.2. Temperature Control and Measurement. A flexible silicone-rubber heating pad with temperature controller (Electro-flex heat EFH-SH-6×9-5-115, Bloomfield, CT, USA) is attached to the outer wall of the testing cell to control the fluid temperature. The heating pad has a nominal maximum temperature of 232℃. Insulation material is wrapped around the cell to prevent heat loss. Figure 3.3 shows the picture of the cell with heating pad and the picture of the cell with insulation.

The actual temperature of the fluid inside the cell is measured by the thermocouple probe (Omega M12JSS-1/8-U-6-D, Stamford, CT, USA). The probe is connected to the thermocouple temperature recorder (Omega OM-CP-QUADTEMP-A, Stamford, CT, USA) and the recorder is then connected to a computer for data acquisition and analysis. The maximum reading rate is 4 Hertz and the probe has an accuracy of ±0.01℃.

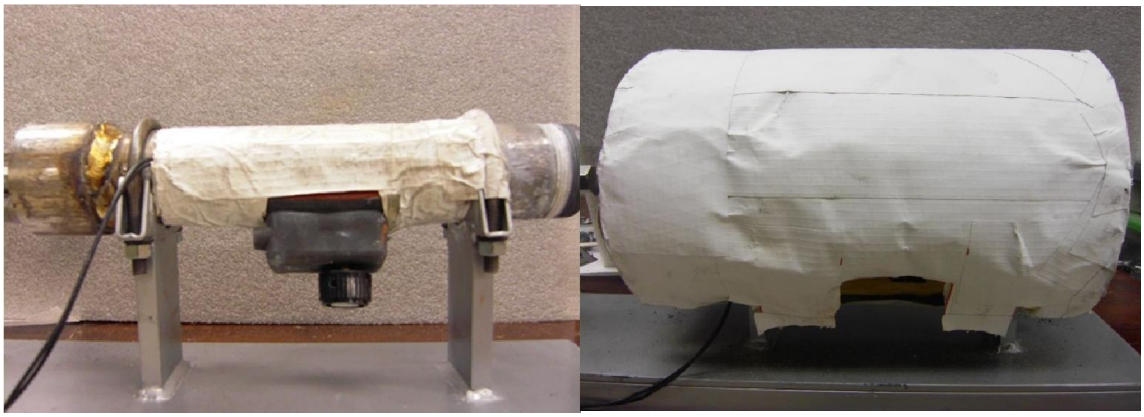

(a) (b)

Figure 3.3 Picture of HPHT Cell Temperature Control System.

3.1.3. Pressure Control and Measurement. The pressurizing of the testing cell is controlled by a pump (Teledyne Isco 100DX, Lincoln, NE, USA) which has a maximum pressure rating of 10,000 psia and a specification of ±1 psia. The pump is able to maintain the cell pressure constant. A pressure transducer (Omega PX409-5.0KGUSBH, Stamford, CT, USA) is used to monitor and transmit the real-time pressure data inside the cell, which has a specification of 0.08% F.S. and a maximum reading rate of 1000 samples/sec. The pressure transducer is then connected to a computer for data acquisition and analysis.

3.1.4. Strain Control and Measurement. Figure 3.4 shows the strain measurement system. The cable will be fixed with the cable fixer and force can be loaded or unloaded with the winch (Shelby Industries 5403C-24Z, Shelbyville, KY, USA). A force gauge is connected between the winch and the cable fixer to monitor the force loaded on cable to make sure the force is within the range of cable endurance. The maximum displacement that can be created on cable is 5 cm. The displacement of cable is measured by the LVDT (Omega LD630-10, Stamford, CT, USA) mounted on top of the cable fixer and connected to computer.

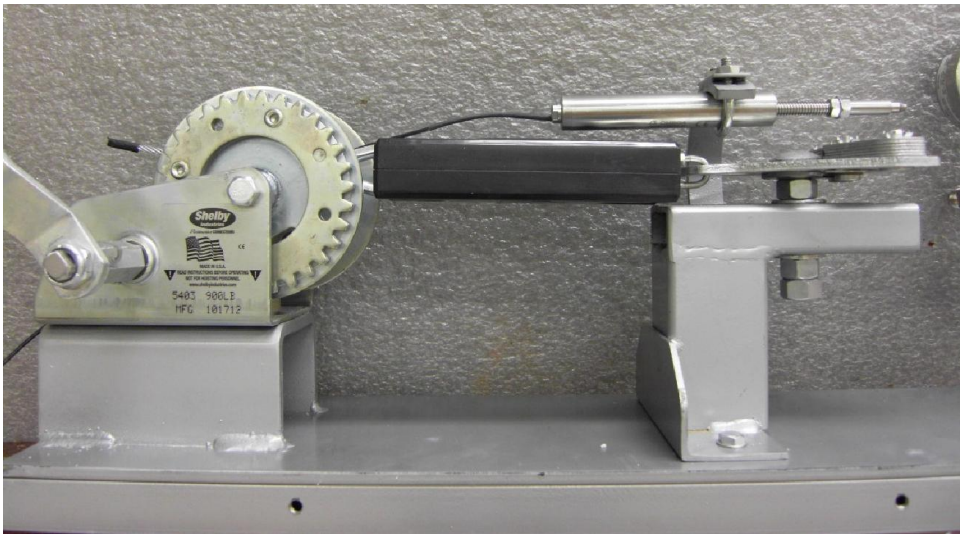

Figure 3.4 Picture of Strain Measurement System.

3.1.5. Sensor Data Acquisition and Analysis. The coaxial cable is connected to a vector network analyzer (VNA HP 8753ES, Santa Clara, CA, USA) which generates the RF signal and monitors the reflection spectrum. The VNA is automatically controlled by a computer running a specifically developed software developed in Matlab^{TM} which can record the spectrum and calculate the shift of minimum wave or mass center of the interferogram.

3.1.6. Operation Safety. Since the test will be dealing with fluids with very high temperature and pressure, especially there is a chance that the cable will be pulled apart during strain test, the procedures established in the previous section should be followed strictly. Besides, a polycarbonate shield is used for safety concern in case that the hot fluid shoots from the hole when the failure of the cable occurs.

3.1.7. Pretest of the HPHT Sensor Testing System. A pretest was conducted on the system to examine the functionality and efficiency of the system. The cell was first pressurized to 5000 psia with water and then the cell was heated at the maximum rate for 5 minutes with the insulation off. The reading rate of the thermocouple probe was set to be every 15 seconds and the recorded temperature showed an increase from 24℃ to 50℃. The heating pad was then turned off and the cell was left in the air for cooling down. After 30 minutes the temperature dropped from 50℃ to 45℃. The cell was then left in air for 24 hours for sealability test. The reading rate of the pressure

transducer was set to be 5 samples/sec. No leakage was detected in the system after 24 hours and the data recorded by the pressure transducer showed that the pressure remains 5000 ± 2 psia over the 24 hour period.

The pretest showed that the system is able to fulfill the objective of testing sensors under various temperature and pressure conditions. The heating can be well controlled by the heating pad and the thermocouple probe can provide the real-time temperature data inside the cell. Although air cooling takes a long time for the cell temperature to go down, it is efficient enough for the test and is the easiest way to operate. The cell showed good sealability and the pump is able to maintain the cell pressure constant over a period long enough for the test.

3.2. CHARACTERIZATION OF COAXIAL CABLE TEMPERATURE SENSOR

A semi-rigid coaxial cable temperature sensor was made and tested under various temperatures at atmospheric pressure (14.7 psia), 84.7 psia and 214.7 psia, respectively, with water being the pressurized fluid environment. Temperature was increased in steps from room temperature to the boiling point at each testing pressure. The VNA scanning rate was set at every 15 seconds which is the same as the thermocouple probe reading rate. In the test at atmospheric pressure, both the shift of the minimum wave and the shift of mass center of the recorded spectrum were calculated and compared, and the one showed a better result was selected as data analysis method for later tests.

3.2.1. Fabrication of Coaxial Cable Temperature Sensor. The coaxial cable used for sensor fabrication is UT-141C-Form-LL cable manufactured by MICRO-COAX®. The specification of the cable is attached in Appendix B.

A coaxial cable Bragg Grating (CCBG) temperature sensor should be fabricated by drilling non-through holes of equal distance into a coaxial cable using diamond drill bit and the filling the hole with high temperature dielectric materials (e.g., alumina) to create periodic impedance discontinuities. In the following tests, the sensor was made in a simplified way in order to test the sensor ability to withstand a combined pressure and temperature environment. Two compressions were made on the cable to work as impedance discontinuities. The distance between the compression centers is 159.6 mm. The end of the cable that goes into the HPHT cell was soldered to prevent any liquid entering the cable under high pressure. Figure 3.6 shows the

simplified coaxial cable temperature sensor. As shown in Figure 3.5, two reflections can be clearly observed with equal reflectivity of 11%. The reconstructed interferogram in spectrum domain has a fringe visibility up to 40 dB.

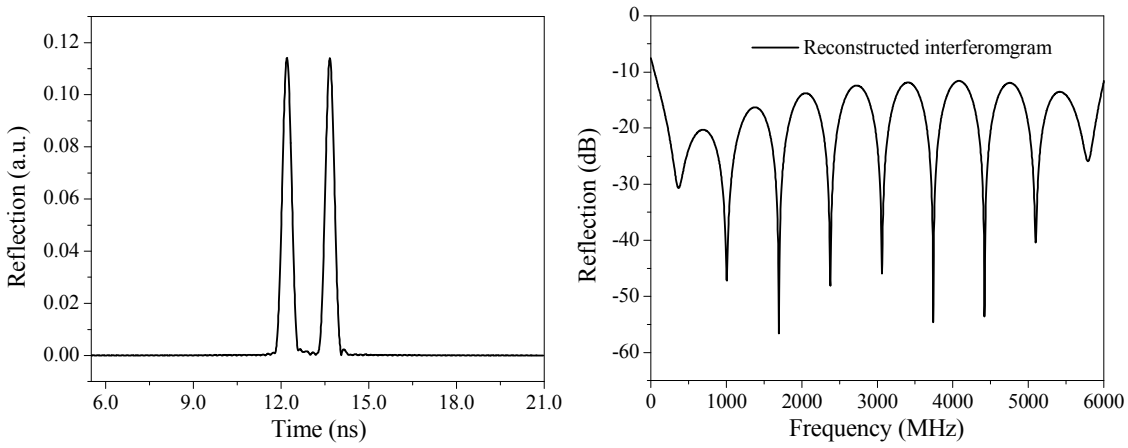

(a) (b)

Figure 3.5 Reconstructed Interferogram of a Semi-Rigid Coaxial Cable Temperature Sensor. (a) Time domain signal, (b) Spectrum domain signal.

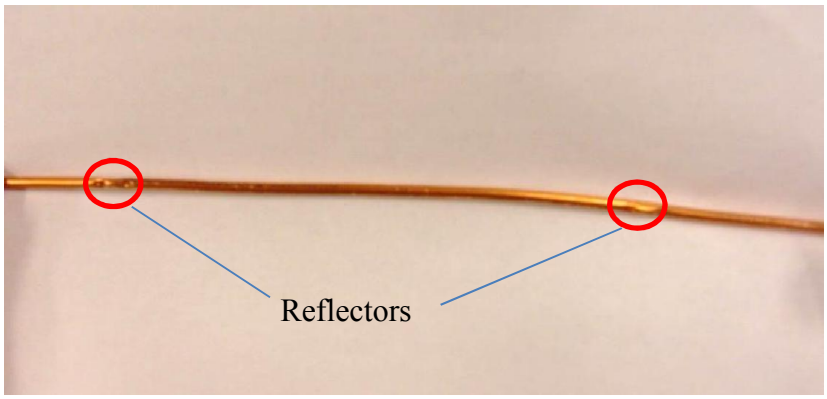

Figure 3.6 Picture of Simplified Coaxial Cable Temperature Sensor.

3.2.2. Test at Atmospheric Pressure (14.7 PSIA). Figure 3.7 shows the cell temperature vs. time and resonant frequency vs. time plots with wave min method in test at atmospheric pressure (14.7 psia). In Figure 3.7 (b), the data between 200 minutes and 300 minutes fluctuate to a very large extent, which doesn't show a good consistency with the cell temperature. In order to mitigate the influence of noise, a low-pass filter is applied to the data. The result after the application of low-pass filter is shown in Figure 3.7 (c). It is clear that large fluctuation still exists.

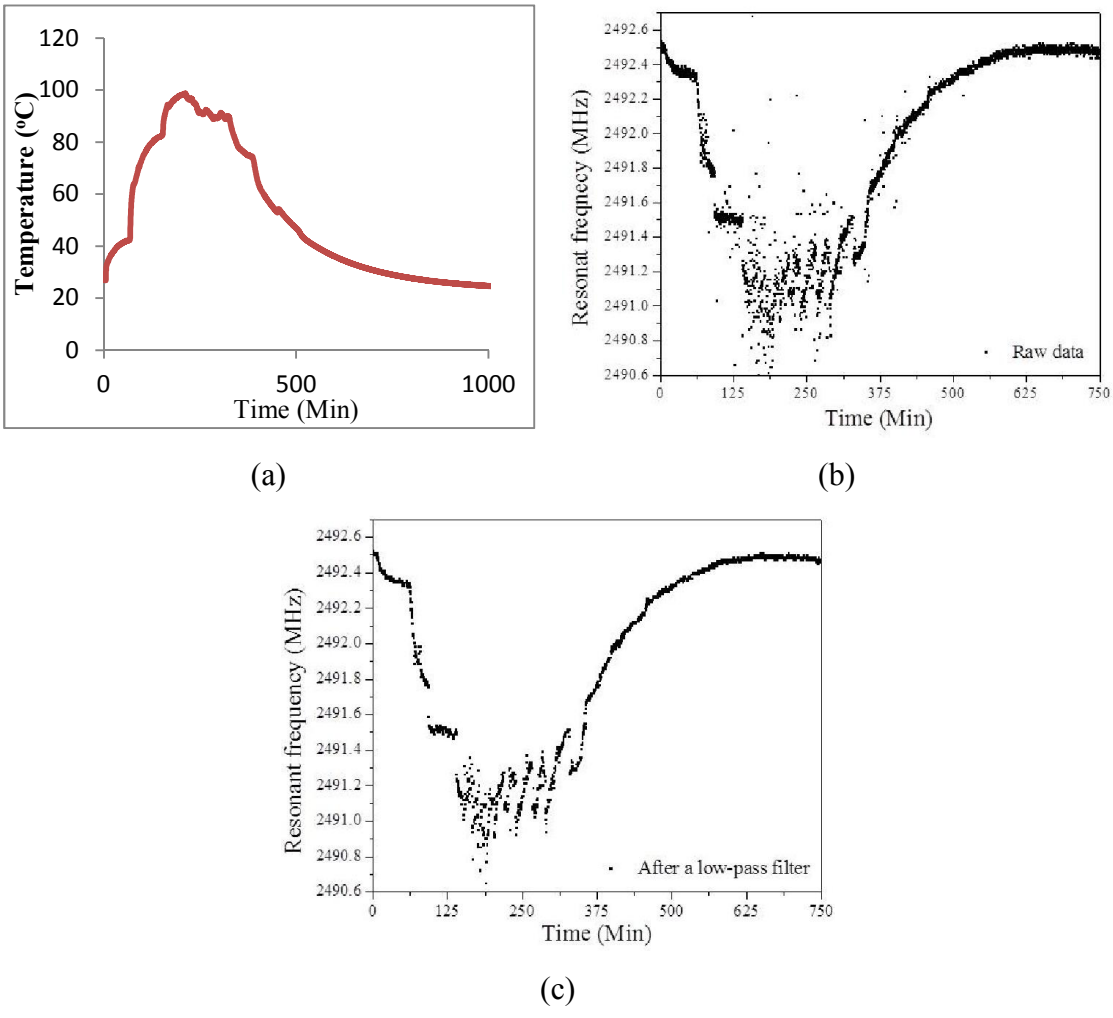

Figure 3.7 Test Results at Atmospheric Pressure (14.7 PSIA) with Wave Min Method.

Figure 3.8 shows the cell temperature vs. time and curve center of mass shift vs. time plots with mass center method in test at atmospheric pressure (14.7 psia). A very good consistency is indicated in these two figures, which means that the sensor was reflecting the actual temperature change in the cell. The standard deviation was analyzed for data between 180 minutes and 240 minutes, as shown in Figure 3.8 (c). The results show that the measurement resolution of the sensor is ±1℃.

Comparing the results of wave min method and the results of mass center methods leads to a clear evidence that the mass center method exhibits a better performance with regard to temperature sensor data analysis. This conclusion results in the use of the mass center method in later tests at 84.7 psia and 214.7 psia.

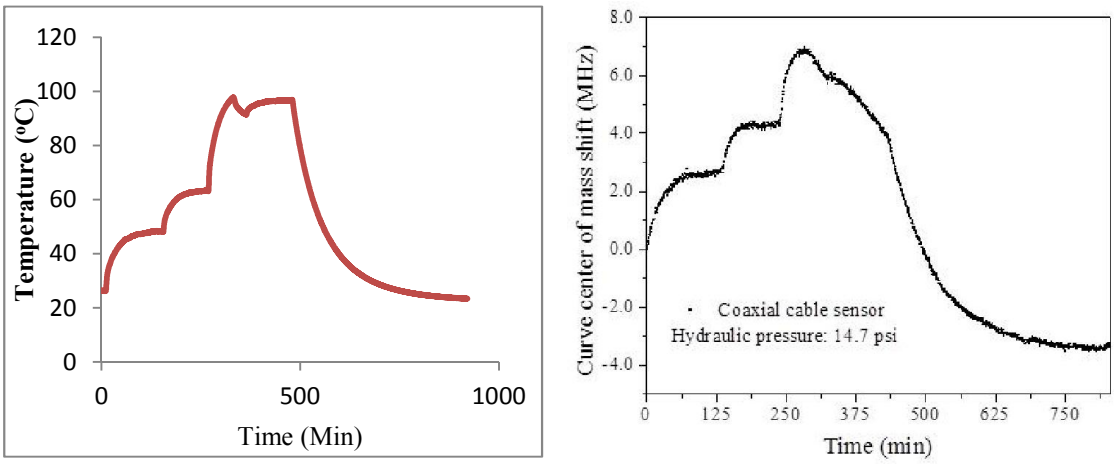

(a) (b)

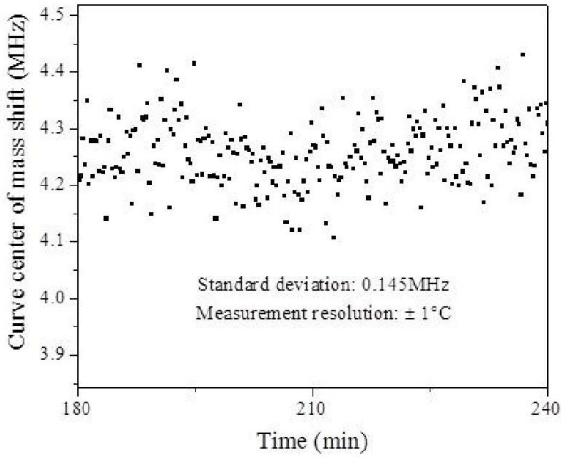

(c)

Figure 3.8 Test Results at Atmospheric Pressure (14.7 PSIA) with Mass Center Method.

3.2.3. Test at 84.7 PSIA. Based on the test results showed in the test at atmospheric pressure, a second test was performed with mass center method at 84.7 psia. Figure 3.9 shows the cell temperature vs. time and curve center of mass shift vs. time plots in test at 84.7 psia. The standard deviation analysis shows that the sensor measurement resolution remains ±1℃ despite the increase of test pressure and temperature range.

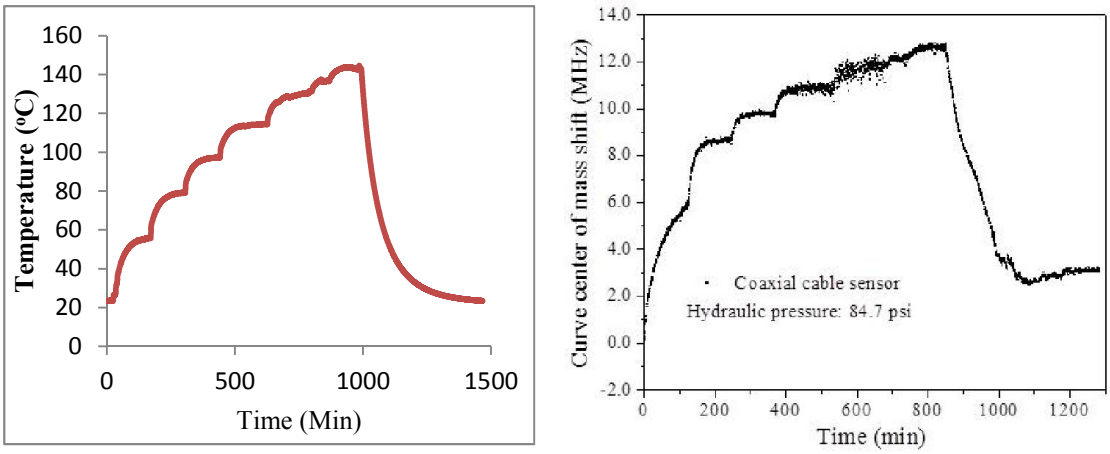

(a) (b)

Figure 3.9 Test Results at 84.7 PSIA with Mass Center Method.

3.2.4. Test at 214.7 PSIA. The test at 214.7 psia was not completed successfully due to the water entering the cable from the cable end. The test was stopped shortly after abnormal results showed up. Figure 3.10 shows the cell temperature vs. time and curve center of mass shift vs. time plots in test at 214.7 psia. The sensor indicated temperature change is not consistent with the actual temperature change in cell, which is increasing. On contrary, the sensor showed a decreasing temperature tendency in the cell.

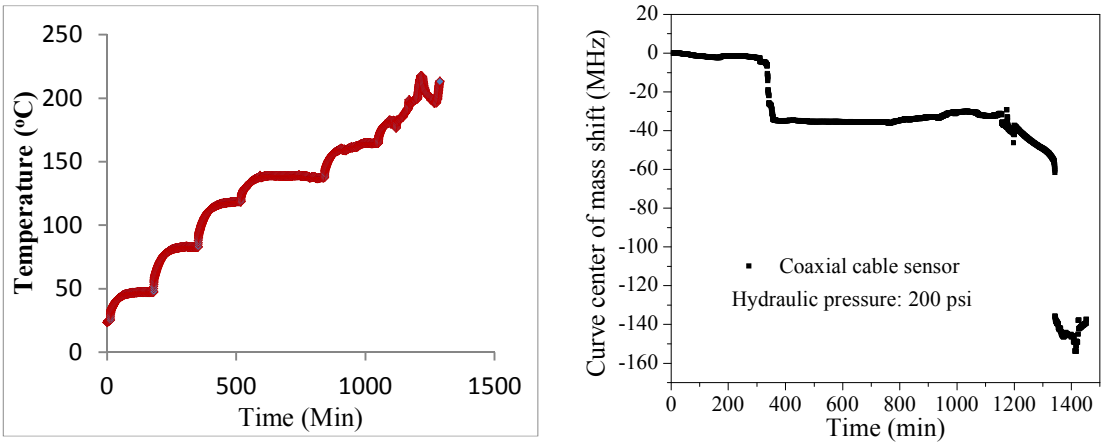

(a) (b)

Figure 3.10 Test Results at 214.7 PSIA with Mass Center Method.

The pressure was released and the coaxial cable sensor was free from the cell. After careful examination of both the cable and the VNA, the cable was found to be integrated from outside; however, a minor amount of water was found in the cable-VNA connector, which might have caused the abnormal test results. Figure 3.11 shows the picture of the coaxial cable sensor after the test at 214.7 psia. The cable was assumed to be working in well condition at least under 1000 psia. The conclusion about the failure of the test is that water entered the cable from the cable end under high pressure due to the inefficient package operation and traveled all the way along the cable to the cable-VNA connector to intervene the signal transmission.

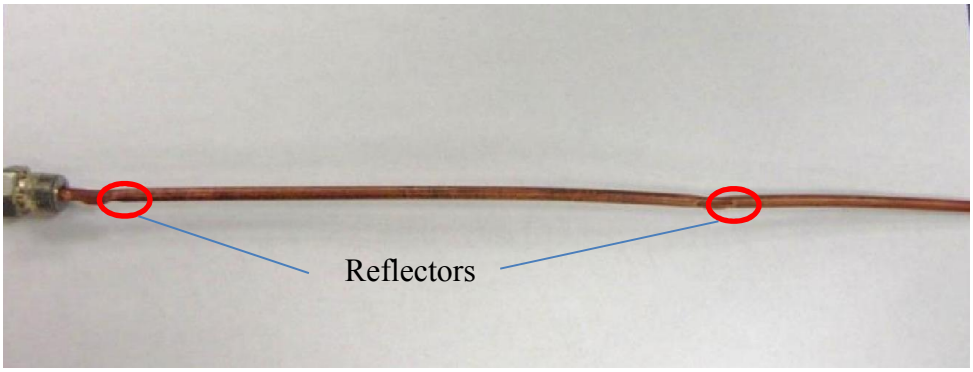

Figure 3.11 Picture of Simplified Coaxial Cable Temperature Sensor after Test at 214.7 PSIA.

3.3. PRELIMINARY TEST ON COAXIAL CABLE PRESSURE SENSOR MODEL

A test was conducted on the coaxial cable pressure sensor model in water under room temperature and zero strain to help with its design. The cable used in this test is made by Cross RF® and the specification of the cable is attached in Appendix B. Figure 3.12shows the design of the sensor. The cable coating and outer conductor were cut off. A metal tube was fixed in the cut area and air was working as the filling material in the tube. A key point of this design is to find an appropriate material for the tube which can withstand high pressure but at the same time can be sensitive enough to pressure change so that to create a shift of the interferogram as well.

(a)

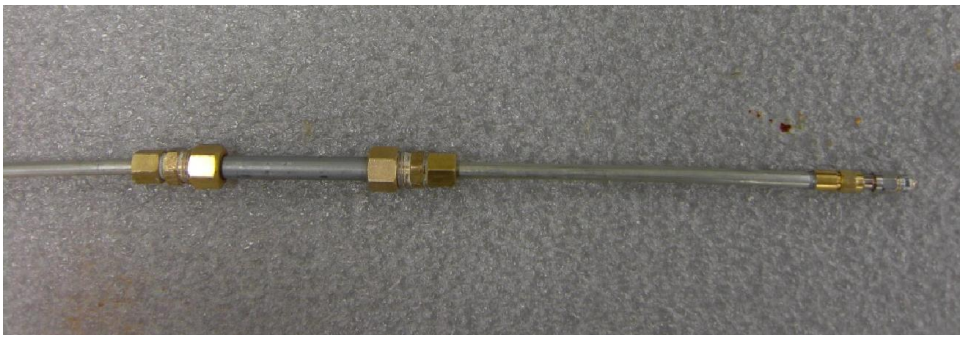

(b)

Figure 3.12 Design of Pressure Sensor Model.

Copper was first used for the metal tube considering that it is soft enough to generate good deformation when pressure is changed. However, in the test it was

observed that when pressure was increased to around 1000psia, water shot from the cable end abruptly. A careful examination of the sensor model showed that the copper tube totally collapsed. Unfortunately copper is too soft to withstand high pressure thus not appropriate to be used in this case.

A steel tube was used instead for a second test. No leakage or collapse was observed when pressure was increased to 5000psia. The system was set for 24 hours at 5000psia and the sensor model showed great survivability. The result showed that a stainless steel tube is a feasible option for material to be used in the pressure sensor.

4. DISCUSSION

4.1. TEMPERATURE CONTROL

Although the current temperature control and measurement system showed a good performance in the tests that have been conducted, a few drawbacks still exist and some improvements need to be made with regard to the system in order to better characterize the sensors for later tests. Since the temperature will reach constant only when the heating and heat loss processes are balanced, the final temperature will always be lower than what is marked on the controller dial, which makes it hard to predict what the final temperature will be and further causes some difficulties in increasing the temperature in a constant step. Besides, it takes a very long period of time for the temperature to reach constant each time the temperature is increased. As can be seen in Figure 3.8 and Figure 3.9, it took 2-3 hours for the temperature to reach final constant status and the step for each temperature increase varied each time.

A new temperature controller (Omega CN7553, Stamford, CT, USA) will replace the old one for better temperature control. A thermocouple will be attached to the outer wall of the HPHT testing cell and the controller will be able to adjust the heating speed automatically according to the preset temperature and the monitored temperature from the thermocouple so that the outer wall of the cell will remain a comparatively constant temperature. This will make the system to reach a more constant temperature which is close to what is expected. The heating speed, however, cannot be predicted to be faster until the new system is tested.

The cooling of the system is another issue that needs to be addressed. Air cooling is an easy way to operate, and with the new temperature controller, it is feasible to realize step decrease of the temperature. However, the time it takes for the fluid to drop to the expected temperature is protracted, which extended the time for each test. Different cooling methods will be tested, such as a tube wrapped around the testing cell with circulating cold water.

4.2. STRAIN CONTROL AND MEASUREMENT

An assumption was made in the strain sensor evaluation which assumes that the sensor thermal expansion under the same temperature and pressure condition remains the same regardless of the mechanical force. The extent of the influence of

mechanical force on cable thermal expansion remains to be determined. The uncertainty of this influence increases the potential inaccuracy of the strain evaluation system. New strain evaluation method needs to be developed if the influence of the mechanical force is found to cause a large inaccuracy in strain evaluation.

4.3. FABRICATION OF COAXIAL CABLE TEMPERATURE SENSOR

The semi-rigid coaxial cable temperature sensor under test was made in a simplified way, which resulted in a lower resolution compared with the temperature sensor made with a more complicated technique. The result of the tests at 14.7 psia (atmospheric pressure) and 84.7 psia showed that the resolution of the temperature sensor being tested is ±1℃. However, future design of the coaxial cable temperature sensor showed a resolution of ±0.1℃ in the test in air, where the sensor was made by drilling holes in the cable and filling the hole with dielectric material (Huang J., personal communication, November 23, 2013). Sensors made with ceramic coaxial cable and the fabrication technique mentioned above have not been tested with the current set up.

4.4. PACKING OF CABLE AND SENSOR

The failure of the test at 200 psia proved the importance of a reliable and effective cable package. Any damage or failure occurred on the cable package may result in the entering of fluid into the cable under high pressure, which may intervene in the signal and travel along the cable to cause fatal damage to the devices. The sensor was found to be intact in the test; however, since the sensor will be made by drilling holes in the cable, a possibility of water ingress into the holes still exists. Thus, a suitable package technique is required for both the cable end and the sensor itself. Soldering is still considered to be a good technique despite the fact that the failed cable was soldered with tin at the end, because it is supposed to provide a good seal of the cable under high pressure. The new sensors will be soldered at the cable end to ensure that no fluid will enter the cable when confined under high pressure.

4.5. CERAMIC COAXIAL CABLE PRESSURE SENSOR JACKET MATERIAL

The preliminary test on ceramic coaxial cable pressure sensor model decided stainless steel to be the proper material for sensor jacket. However, although the stainless steel tube showed great performance in maintaining integrity under high pressure, the sensitivity of the pressure sensor still needs to be tested. Stainless steel has a high Young's modulus and is not so easy to be deformed under high pressure, which can reduce the sensitivity of the pressure sensor. New materials have to be tested if the stainless steel cannot provide sensitivity high enough for the intended application.

4.6. SYSTEM IMPOSED NOISES

Theoretically, the resonance is merely caused by the two reflections, which are the two compressions made on the semi-rigid coaxial cable. However, additional resonance may exist due to the inherent defects of the system. The cable end and the inlet cap cable fastener can perform as reflections. The cable fixer in strain evaluation system will also cause additional compression on the cable to play as another reflection. These reflections can interfere in the final interferogram and cause difficulties in data analysis. The sensor fabrication technique mentioned in Section 4.3 needs to be used to make sure that the resonant frequency caused by sensor reflections is easier to be distinguished from the frequency caused by the testing system.

In addition to the system imposed reflections, vibration caused by gas bubbles is another factor that can intervene in the interferogram. When temperature increases, gas will escape from the fluid, and the generated bubbles will cause a certain extent of vibration to the cable, which can be a possible factor that will influence the interferogram. Pre-degassed fluid needs be used to help reduce the influence of bubble caused vibration.

4.7. APPLICABILITY OF THE SEMI-RIGID COAXIAL CABLE TEMPERATURE SENSOR

The test results of the simplified semi-rigid coaxial cable temperature sensor indicate the feasibility for downhole temperature monitoring with regard to leak detection. In Prudhoe Bay, Alaska, fiber optic distributed temperature surveys are used as a leak detection method (Julian et al. 2007). The typical temperature

resolution for a 8,000 ft well is 1℉ at the bottom of the well for a single-ended measurement (measure the reflection of the applied signal). Out of the twelve wells under investigation, leakage of ten wells were successfully detected and identified with the fiber optic distributed survey, including tubing leak, production casing leak, packer leak, leaking sand plug and leaking tubing straddle. In the tests conducted in this research, the semi-rigid coaxial cable temperature sensor was interrogated by measuring the reflection of the applided signal, and it showed a constant measurement resolution of ±1℃ from room temperature to the boiling point of water at 14.7 psia and 84.7 psia, respectively, which indicate that the sensor can be used for downhole leak detection.

In addition, the developed semi-rigid coaxial cable temperature sensor is also found possible to be used in short time interval CO_2 leak detection and long-term reservoir CO_2 saturation change. A mathematical model studied the temperature signal as a function of CO_2 saturation (Hurter el al. 2007). The result showed that the effect of a rock section with high CO_2 saturation is to increase the geothermal gradient and shift the temperature below the CO_2 enriched layer upwards in an order of a few degrees Celsius. And moving CO_2 would cause easily detected temperature anomalies of up to tens of degrees Celsius. The resolution of the semi-rigid coaxial cable temperature sensor can sense the corresponding temperature change so that it can be used to track the CO_2 plume movement and detect CO_2 leakage.

5. CONCLUSIONS

A HPHT sensor testing system has been designed and fabricated in order to characterize the ceramic coaxial cable sensors under combined temperature, pressure and strain conditions. The testing range of the sensors was determined through considering the field operational range and the expected sensor range as well as the accessible equipment and manufacturing techniques. A pretest was performed on the system with water and the system showed a good performance in temperature and pressure control and measurement as well as sealability.

A simplified semi-rigid coaxial cable temperature sensor was manufactured and tested under combined temperature and pressure conditions. Two compressions distanced at 159.6 mm were made on the cable as reflections. Two sets of tests were smoothly conducted with water from room temperature to the boiling point of water at 14.7 psia (atmospheric pressure) and 84.7 psia, respectively. Both wave min method and mass center method were used in the test at 14.7 psia as a way of data interpretation, and the mass center method showed a better result, which made it the selected data interpretation method in later tests. The test results show that the sensor is able to monitor the actual temperature of hydraulic water with a resolution of ±1℃. Test at 214.7 psia failed owning to the intervention of water entered from the cable end and transported to the cable-VNA connector. It proved that good package technique is required to prevent any liquid ingress under extreme pressure.

The preliminary test of ceramic coaxial cable pressure sensor model decided stainless steel as the proper material for sensor jacket. Copper was first considered due to its ductility and a copper tube based sensor model was tested with hydraulic water at room temperature, but the copper tube totally collapsed when the pressure increased to 1000 psia. A second test was run with a stainless steel tube, and it remained intact at 5000 psia after 24 hours.

6. FUTURE WORK

A series of work will be conducted in the following quarters of this project in order to fulfill the objectives stated in Section 1.4. The planned work includes improving the performance of the HPHT sensor testing system, fabrication of new ceramic coaxial cable temperature sensors with a more complex technique, design and fabrication of ceramic coaxial cable pressure sensor, test on the ceramic coaxial temperature, strain and pressure sensors with water, brine, oil, CO_2 and CO_2/brine mixture, and test on sensor long-term stability and survivability with cyclic heating and cooling of the testing system.

Part of the HPHT sensor testing system will be modified or replaced so that to improve the temperature control performance and strain measurement accuracy. The currently used temperature controller will be replaced with a new programmable temperature controller (Omega CN7553, Stamford, CT, USA). The new temperature controller works by changing the heating rate based on the input temperature data which is collected by the thermocouple attached to the outer wall of the testing cell, so that the fluid will be able to remain at a desire temperature. And the programmable feature of the temperature controller requires far less effort to change the cell temperature compared to the manually operated one. Besides, new strain measurement method will be designed and tested in order to correct the assumption that the strain caused by thermal expansion remains the same regardless of the existence of mechanical force.

New ceramic coaxial cable temperature, strain and pressure sensors will be fabricated and tested. Ceramic coaxial cable temperature and strain sensors will be fabricated by drilling evenly distributed non-through holes into the cable and filling the hole with high temperature dielectric material or metal. In addition, the research group from Clemson University is intensely working the design and fabrication of the ceramic coaxial cable pressure sensor. Once the sensors are finished, a series of tests will be conducted to test the sensor short-term performance under combined temperature, pressure and strain conditions with water. Later, the tests will be performed with different fluids such as brine, oil, CO_2 and CO_2/brine mixture to establish a sensor performance matrix. Finally, the sensor long-term stability and survivability will be tested by cyclic heating and cooling of the system.

APPENDIX A.
SPECIFICATIONS OF THE HPHT SENSOR TESTING EQUIPMENT

Table A.1. Specifications of HPHT Sensor Testing Equipment.

Part Name	Brand	Model Number	Material	Dimension
HPHT Testing Cell	-	-	Stainless Steel	Inner Diameter: 5 cm Outer Diameter: 10 cm Length: 30 cm
Heating Pad	Electro-Flex Heat	EFH-SH-6×9-5-115	-	6 in × 9 in
Temperature Controller	Electro-Flex Heat	-	-	-
Pressure Transducer	Omega	PX409-5.0KGUSBH	-	-
LVDT	Omega	LD630-10	-	-
Pump	Teledyne Isco	100DX	-	-
High Pressure Pipeline	-	-	-	1/8 in
Winch	Shelby Industries	5403C-24Z	-	-
Thermocouple Probe	Omega	M12JSS-1/8-U-6-D	-	-
Temperature Recorder	Omega	OM-CP-QUADTEMP-A	-	-
Cell Insulation	-	-	Fiber Glass	Thickness: 5cm
VNA	Hewlett Packard	8753ES	-	-

APPENDIX B.
SPECIFICATIONS OF COAXIAL CABLES USED IN TESTS

Table B.1. Specifications of UT-141C-Form-LL Coaxial Cable by MICRO-COAX®.

DIMENSIONS		
Jacket Diameter (mm)	-	
Outer Conductor Diameter (mm)	3.581	
Dielectric Diameter (mm)	2.896	
Wire Diameter (mm)	0.889	
MATERIALS		
Wire	SPC	
Dielectric	LD PTFE	
Outer Conductor	Tin-Dipped Braid	
Jacket	-	
RoHS Compliant	YES	
MECHANICAL CHARACTERISTICS		
Maximum Temperature (℃)	225	
Bend Radius (mm)	12.7	
Weight (grams/m)	40.7	
ELECTRICAL CHARACTERISTICS		
Characteristic Impedance (ohms)	50	
Capacitance (Nominal) (pF/m)	88.6	
Velocity of Propagation (%)	77%	
Maximum Voltage, VRMS	1900	
Signal Delay (ns/m)	4.33	
Frequency Range	DC-20	
Typical Attenuation (dB/100ft)/Average Power (Watts CW) @ 20℃ Sea Level	0.5 GHz	9
	1.0 GHz	12
	10.0 GHz	48
	18.0 GHz	71

Table B.2. Specifications of LL-335 Coaxial Cable by Cross RF®.

Physical Characteristics		
Center Conductor Diameter (in)		.08 Solid
Dielectric Diameter (in)		.250
Diameter Over Inner Braid (in)		.258
Diameter Over Interlayer (in)		.264
Diameter Over Outer Braid (in)		.284
Overall Diameter (in)		.335
Weight (lbs./MFT)		124
Operating Temperature Range(℃)		-55 +200
Min .Recommended Bend Radius (in)		1.7
Electrical Characteristics		
Impedance (Ohms)		50
Capacitance (pF/ft.)		25.0
Velocity of Propagation (%)		80
Attenuation (dB/100ft) (Typ. / Max.)	@ 400 MHz	2.4 / 3.5
	@ 1 GHz	4.8 / 5.5
	@ 2 GHz	6.8 / 7.8
	@ 3 GHz	8.4 / 9.5
	@ 5 GHz	10.3 / 12.5
	@ 10 GHz	17.0 / 19.0
	@ 18 GHz	22.0 / 26.0
Cut-off Frequency (GHz)		18.0
Shielding Effectiveness		> -90 dB

APPENDIX C.
GEOLOGIC CO_2 SEQUESTRATION MONITORING COST ANALYSIS

Cost is one of the primary concerns when considering if a certain monitoring technique will be adopted in a CO_2 sequestration project. Table C.1 is a monitoring unit costs analysis provided by the EPA in 2010. Significant components of potential monitoring costs include the drilling of monitoring wells above and into the injection zone, implementation of the subsurface and surface monitoring, and periodic seismic surveys and reservoir modeling.

Table C.1. Monitoring Unit Costs.

Cost Reporting Heading	Unit Cost Heading	Tracking Number	Cost Item	Cost Algorithm	Data Sources
Monitoring	Site Selection and Evaluation	B-1	Develop geochemical baseline for injection zones and confining zone.	$200 per sample. Assume 4 samples per injection well = $800 per injection well	Lab analysis fee of $100 to $200 discussed in N.O. meeting.
Monitoring	Site Selection and Evaluation	B-2	Develop baseline of surface air CO2 flux for leakage monitoring.	$35,000 per station	Range of costs discussed at N.O. meeting Jan 2008 was $20,000 to $50,000 per station.
Monitoring	Site Selection and Evaluation	B-3	Conduct front-end engineering and design (monitoring wells)	$20,000 + $5,000/shallow monitoring well	ICF estimate.
Monitoring	Land and Land Use Rights	B-4	Obtain rights-of-way for surface uses. (monitoring wells)	$10,000 per monitoring well site	ICF estimate. Cost of land rights are highly variable.
Monitoring	Land and Land Use Rights	B-5	Obtain rights-of-way for surface uses. (monitoring sites)	$5,000 per air monitoring station site (microseismic is done inside montoring well)	ICF estimate. Cost of land rights are highly variable.
Monitoring	Drilling and Equipping Injection Wells	B-6	Downhole safety shut-off valve	$15,000 + $2/ft depth. Would be placed 100 or more feet above packer	Initial cost estimate until more data are obtained.
Monitoring	Drilling and Equipping Monitoring Wells	B-7	Standard monitoring well cost (ABOVE injection zone)	Use look-up table. $/foot = $100 to $130 per foot typical for **slim-hole design** down to 9,000 ft.	Drilling cost is estimated fom drilling cost equations developed from JAS and PSAC data.
Monitoring	Drilling and Equipping Monitoring Wells	B-8	Standard monitoring well cost (INTO injection zone)	Use look-up table. $/foot = $100 to $130 per foot typical for **slim-hole design** down to 9,000 ft.	Drilling cost is estimated fom drilling cost equations developed from JAS and PSAC data.
Monitoring	Downhole Monitoring Equipment (for Monitoring Wells or Injection Wells)	B-9	Pressure and temperature gauges and related equipment for monitoring wells	$10,000/well	Initial cost estimate until more data are obtained.
Monitoring	Downhole Monitoring Equipment (for Monitoring Wells or Injection Wells)	B-10	Salinity, CO2, tracer, etc. monitoring equipment for wells (portion of equipment may be at surface such as for *in situ* sampling using U-tubes)	$10,000/well	Initial cost estimate until more data are obtained.
Monitoring	Surface or Near-Surface Monitoring Equipment	B-11	Develop plan and implement surface air and/or soil monitoring within current plume footprint	40 hours @$106.31/hr = $4252 for plan plus $70,000/monitoring site	ICF estimate of time required. Hourly rate may change based on labor survey data. Monitoring station cost estimate from Benson 2004.
Monitoring	Surface or Near-Surface Monitoring Equipment	B-12	Develop plan and implement surface air and/or soil monitoring within current plume footprint, at artificial penetrations and sensitive locations (human occupancy)	40 hours @$106.31/hr = $4252 for plan plus $70,000/monitoring site	ICF estimate of time required. Hourly rate may change based on labor survey data. Monitoring station cost estimate from Benson 2004.
Monitoring	Surface or Near-Surface Monitoring Equipment	B-13	Surface microseismic detection equipment	$50,000/ site (geophone arrays go into monitoring wells)	Initial cost estimate until more data are obtained.
Monitoring	Operating Costs	B-14	Monitoring well O&M	Annual O&M costs are $25,000 + $3/ft per well per year	Operating and maintenance costs adapted from EIA Oil and Gas Lease Equipment and Operating Cost estimates.
Monitoring	Operating Costs	B-15	Annual cost of air and soil surveys & equipment	$10,000 per station per year	ICF estimate.
Monitoring	Operating Costs	B-16	Annual cost of passive seismic equipment	$10,000 per station per year	ICF estimate.
Monitoring	Operating Costs	B-17	Periodic seismic surveys: 3D	$75,000/square mile for good resolution	Several published reports are in range of this cost.
Monitoring	Operating Costs	B-18	Complex modeling of fluid flows and migration (reservior simulations) every five years	180 hours of engineers @$53.52/hr = $9634 per site + 24 hours of engineers @$53.52/hr = $1284 per injection well	ICF estimate of time required. Hourly rate may change based on labor survey data.
Monitoring	Operating Costs	B-19	Annual reports to regulators	20 hours of engineers @$53.52/hr = $1070 per report	ICF estimate of time required. Hourly rate may change based on labor survey data.
Monitoring	Operating Costs	B-20	Quarterly reports to regulators	15 hours of engineers @$53.52/hr = $803 per report	ICF estimate of time required. Hourly rate may change based on labor survey data.
Monitoring	Operating Costs	B-21	Monthly reports to regulators	8 hours of engineers @$53.52/hr = $428 per report	ICF estimate of time required. Hourly rate may change based on labor survey data.

A monitoring cost estimate of the Wabamun Area Sequestration Project (WASP) shows that the cost of monitoring will make up approximately 75% of the project's total cost (Nygaard & Lavoie 2009). Table C.2 shows the cost summary for four different injection scenarios. It shows that the vertical fractured scenario is more costly than the horizontal injection wells and 4D seismic consists of the largest expense for all scenarios.

Table C.2. Cost Summary for the Four Scenarios Including Total Cumulative Injection.

Cost Item Groups	Scenario 1	Scenario 2	Scenario 3	Scenario 4
	Vertical ($1000 CAD)	Vertical Fracture Stimulated ($1000 CAD)	Horizontal ($1000 CAD)	Horizontal fracture stimulated ($1000 CAD)
Site planning and preparation	1,566	1,566	1,566	1,566
Injection well cost	13,862	14,569	27,538	31,738
Injection well operations	79,085	79,085	79,085	79,085
Well re-abandonment	3,108	3,108	3,108	3,108
Surface monitoring cost	162,090	162,090	162,090	162,090
4D seismic costs	316,341	512,171	466,979	647,746
Monitoring wells costs	11,187	11,187	11,187	11,187
Monitoring well operations	22,046	22,046	22,046	22,046
Equipment replacement	28,786	29,571	43,948	48,610
Surface lease and lease insurance	6,938	6,938	6,938	6,938
Project management, administration, and engineering	39,654	39,654	39,654	39,654
Total Cost	**684,662**	**881,984**	**864,138**	**1,053,767**
Cumulative Injectivity (Million Tons)	**200**	**309**	**282**	**391**

APPENDIX D.

BOILING POINTS OF WATER UNDER DIFFERENT PRESSURES

Since the tests are conducted under combined temperature and pressure conditions, it is essential to know the boiling points of water under different pressure to determine the temperature operating range in each test for both operation safety and cable integrity considerations. As the temperature getting close to the boiling point at the tested pressure, gas would escape from water to make bubbles, therefore result in the vibration of water, which can intervene into the transmission of the signal and cause extra noise. Besides, compared to water the generated gas would more easily enter the cable to cause fatal damage if the cable is not packaged well. The Engineering Toolbox® provides the boiling points of water at pressure ranging from 0.5 psia to 1000 psia as shown in Figure D.1.

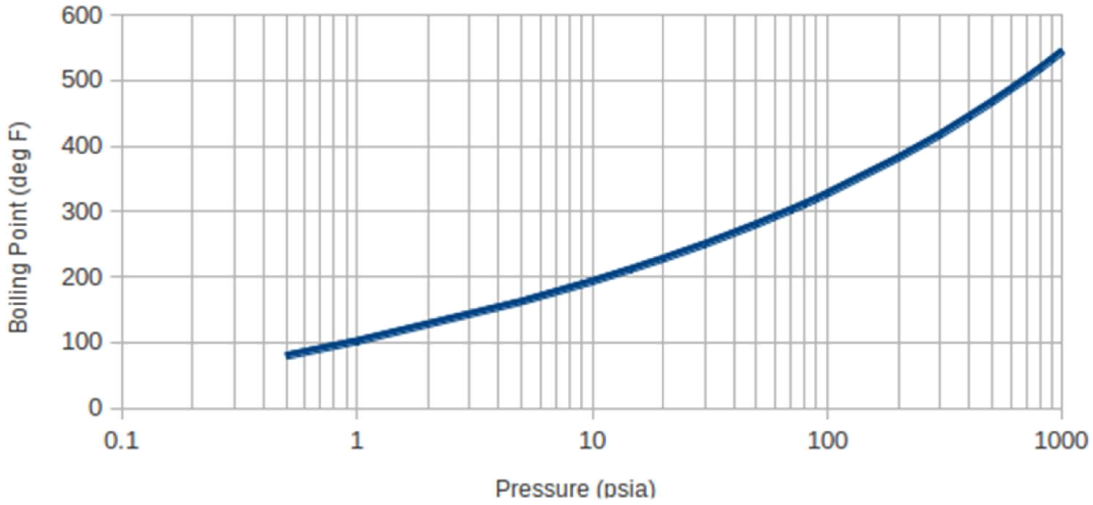

Figure D.1. Boiling Points of Water at Pressure Ranging 0.5–1000 PSIA.

BIBLIOGRAPHY

Avci, C. B. (1994). Evaluation of flow leakage through abandoned wells and boreholes. *Water Resources Research, 30*(9), 2565-2578.

Bachu, S. (2003). Screening and ranking of sedimentary basins for sequestration of CO_2 in geological media in response to climate change. *Environmental Geology*, 44(3), 277-289.

Baker Hughes Incorporated. (2010a). SureView real-time fiber-optic compaction monitoring system [Brochure]. Retrieved July 11, 2013 from http://c14503045.r45.cf2.rackcdn.com/v1/6d9595dc1c7754cdc039ba0ad7cd32e5/30643-real-time-fiber-optic-casing-imaging-system_brochure-0910.pdf.

Baker Hughes Incorporated. (2010b). Optical reality: fiber-optic technology monitors sand screen deformation in real time. *Connexus, 1*(1), 20-23.

Belkin International Incorporated. (2012). The construction of a fiber-optic cable [Online image]. Retrieved April 10, 2013 from http://www.belkin.com/networking/fiber.

Benson, S. M., & Cole, D. R. (2008). CO_2 sequestration in deep sedimentary formations. *Elements*, 4(5), 325-331.

Benson, S. M., Gasperikova, E., & Hoversten, G. M. (2004, September). Monitoring protocols and life-cycle costs for geologic storage of carbon dioxide. In *Proceedings of the 7th International Conference on Greenhouse Gas Control Technologies (GHGT-7)* (pp. 1259-1266).

Brown, G., Carvalho, V., Wray, A., Smith, D., Toombs, M., & Pennell, S. (2004, January). Monitoring alternating CO_2 and water injection and its effect on production in a carbonate reservoir using permanent fiber-optic distributed temperature systems. In *SPE Annual Technical Conference and Exhibition*. Society of Petroleum Engineers.

Cairns, G., Jakubowicz, H., Lonergan, L., & Muggeridge, A. (2010, January). Issues regarding the use of time-lapse seismic surveys to monitor CO_2 sequestration. Society of Exploration Geophysicists.

Castro, R.M., Pascacio, D., Guevara, R., Tello, C., Pacheco, O., Antunez, J., & Martínez, I. (2013, July). Development of HPHT downhole measurements tools: challenges and strategies. In *Petroleum and Chemical Industry Committee Technical Conference*.

Chadwick, R. A., Arts, R., Eiken, O., Kirby, G. A., Lindeberg, E., & Zweigel, P. (2004). 4D seismic imaging of an injected CO_2 plume at the Sleipner Field, central North Sea. Geological Society of London.

Choi, I. M., Woo, S. Y., & Kim, Y. K. (2011). Evaluation of high temperature pressure sensors. *Review of Scientific Instruments, 82*(3), 035112.

Costello, C., Sordyl, P., Hughes, C. T., Figueroa, M. R., Balster, E. P., & Brown, G. (2012, January). Permanent distributed temperature sensing (DTS) technology applied in mature fields - a Forties field case study. Society of Petroleum Engineers. doi:10.2118/150197-MS.

European Commission. (2013, May). State of art report on monitoring technology (Report No. D-N^{o}: 2.2.2). Retrieved October 20, 2013 from http:// www.modern-fp7.eu/fileadmin/modern/docs/Deliverables/MoDeRn_ D2.2.2_State_of_art_report.pdf.

Freifeld, B. M. (2009, January). Integrated well-based monitoring for CO_2 sequestration. Society of Petroleum Engineers. doi:10.2118/127752-MS.

Freifeld, B. M., Daley, T. M., Hovorka, S. D., Henninges, J., Underschultz, J., & Sharma, S. (2009). Recent advances in well-based monitoring of CO_2 sequestration. *Energy Procedia, 1*(1), 2277-2284.

Global CCS Institute. (2014, February). Large-scale integrated CCS projects. Retrieved January 21, 2014 from http://www.globalccsinstitute.com/ projects/browse.

Hovorka, S. D., Benson, S. M., Doughty, C., Freifeld, B. M., Sakurai, S., Daley, T. M., ... & Knauss, K. G. (2006). Measuring permanence of CO_2 storage in saline formations: the Frio experiment. *Environmental Geosciences*, *13*(2), 105-121.

Huang, J., Wang, T., Hua, L., Fan, J., Xiao, H., & Luo, M. (2013). A Coaxial Cable Fabry-Perot Interferometer for Sensing Applications. *Sensors, 13*(11), 15252-15260.

Huang, J., Wei, T., Lan, X., Fan, J., & Xiao, H. (2012, April). Coaxial cable Bragg grating sensors for large strain measurement with high accuracy. In *SPIE Smart Structures and Materials+ Nondestructive Evaluation and Health Monitoring* (pp. 83452Z-83452Z). International Society for Optics and Photonics.

Huang, X., Bandilla, K. W., Celia, M. A., & Bachu, S. (2014). Basin-scale modeling of CO_2 storage using models of varying complexity. *International Journal of Greenhouse Gas Control*, 20, 73-86.

Hurter, S., Garnett, A. A., Bielinski, A., & Kopp, A. (2007, January 1). Thermal signature of free-phase CO_2 in porous rocks: detectability of CO_2 by temperature logging. Society of Petroleum Engineers. doi:10.2118/109007-MS.

Julian, J. Y. (2007, January 1). Downhole leak determination using fiber-optic distributed-temperature surveys at Prudhoe Bay, Alaska. Society of Petroleum Engineers. doi:10.2118/107070-MS.

Karaman, O. S., Kutlik, R. L., & Kluth, E. L. (1996, January). A field trial to test fiber optic sensors for downhole temperature and pressure measurements, West Coalinga field, California. Society of Petroleum Engineers. doi:10.2118/35685-MS.

Katzer, J., Ansolabehere, S., Beer, J., Deutch, J., Ellerman, D., Friedmann, J., ... & Steinfeld, E. (2007). The future of coal: options for a carbon-constrained world. *Massachusetts Institute of Technology*.

Koelman, J. V. (2011). Fiber-optic sensing technology providing well, reservoir information-anyplace, anytime. *Technology update. JPT, 63*(7), 22-24.

Koelman, J. V. V., Lopez, J. L., & Potters, H. (2011, January). Fiber optic technology for reservoir surveillance. *International Petroleum Technology Conference*. doi:10.2523/14629-MS.

Korbol, R., & Kaddour, A. (1995). Sleipner West CO_2 disposal: injection of removed CO_2 into the Utsira formation. *Energy Conversion and Management, 36*(6-9), 509-512.

Lee, B. (2003). Review of the present status of optical fiber sensors. *Optical Fiber Technology, 9*(2), 57-79.

Little, M. G., & Jackson, R. B. (2010). Potential impacts of leakage from deep CO_2 geosequestration on overlying freshwater aquifers. *Environmental science & technology, 44*(23), 9225-9232.

Lüth S., Bergmann P., Giese R., Götz J., Ivanova A., Juhlin C. & Cosma C. (2011). Time-lapse seismic surface and down-dole measurements for monitoring CO_2 storage in the CO2SINK project (Ketzin,Germany). *Energy Procedia, 4*(3435–3442). doi:10.1016/j.egypro.2011.02.268.

Martens, S., Kempka, T., Liebscher, A., Lüth, S., Möller, F., Myrttinen, A., ... & Kühn, M. (2012). Europe's longest-operating on-shore CO_2 storage site at Ketzin, Germany: a progress report after three years of injection. *Environmental Earth Sciences, 67*(2), 323-334.

Medina, M., Torres, C. E., Sanchez, J., Boida, L., Leon, A. J., Jones, J. A., & Yicon, C. (2012, January). Real-Time downhole monitoring of electrical submersible pumps rated to 250 degree C using fiber optic sensors: case study and data value in the Leismer SAGD project. Society of Petroleum Engineers. doi:10.2118/153984-MS.

Molenaar, M. M., Fidan, E., & Hill, D. J. (2012, March). Real-time downhole monitoring of hydraulic fracturing treatments using fibre optic distributed temperature and acoustic sensing. In *SPE/EAGE European Unconventional Resources Conference & Exhibition-From Potential to Production*.

Molenaar, M. M., Hill, D., Webster, P., Fidan, E., & Birch, B. (2011, January). First downhole application of distributed acoustic sensing (DAS) for hydraulic fracturing monitoring and diagnostics. Society of Petroleum Engineers. doi:10.2118/140561-MS.

Nordbotten, J. M., Celia, M. A., & Bachu, S. (2004). Analytical solutions for leakage rates through abandoned wells. *Water Resources Research, 40*(4), W04204.

Nordbotten, J. M., Celia, M. A., & Bachu, S. (2005). Injection and storage of CO_2 in deep saline aquifers: Analytical solution for CO_2 plume evolution during injection. *Transport in Porous media, 58*(3), 339-360.

Nygaard, R. & Lavoie, R. (2009). Project cost estimate-Wabamun area CO_2 sequestration project (WASP). University of Calgary.

Nygaard, R., Bai, B., & Eckert, A. (2013, February). Geomechanical simulation of CO_2 leakage and cap rock remediation. Rolla, MO: Missouri University of Science and Technology.

Pan, Y., Chen, Z., Xiao, L., Zhang, Y., & Fu, J. (2010, July). Application of fiber Bragg grating sensor networks in oil wells. In *Nigeria Annual International Conference and Exhibition*.

Pawar, R. J., Warpinski, N. R., Benson, R. D., Grigg, R. B., Krumhansl, J. L., & Stubbs, B. A. (2004, January). Geologic Sequestration of CO_2 in a Depleted Oil Reservoir: An Overview of a Field Demonstration Project. Society of Petroleum Engineers. doi:10.2118/90936-MS.

Ringrose, P., Atbi, M., Mason, D., Espinassous, M., Myhrer, Ø., Iding, M., ... & Wright, I. (2009). Plume development around well KB-502 at the In Salah CO_2 storage site. *First Break, 27*(1).

Sakurai, S., Ramakrishnan, T. S., Boyd, A., Mueller, N., & Hovorka, S. (2006). Monitoring saturation changes for CO_2 sequestration: petrophysical support of the Frio brine pilot experiment. *Petrophysics, 47*(6), 483-496.

Schmidt-Hattenberger, C., Otto, P., Toepfer, M., Borm, G., & Baumann, I. (2004, June). Development of fiber Bragg grating (FBG) permanent sensor technology for borehole applications. In *Second European Workshop on Optical Fibre Sensors* (pp. 124-127). International Society for Optics and Photonics.

Tardy, P., Chang, F., & Qiu, X. (2011, November). Determining Matrix Treatment Performance From Downhole Pressure And Temperature Distribution: A Model. In *International Petroleum Technology Conference*.

The National Energy Technology Laboratory. (2009). Project solicitation innovative and advanced technologies and protocol for monitoring/verification/ accounting (MVA), simulation, and risk assessment of carbon dioxide (CO_2) sequestration in geologic formations. United States Department of Energy.

The National Energy Technology Laboratory. (2012). Project S national energy technology laboratory, technologies to ensure permanent geologic carbon storage. United States Department of Energy.

Thermocoax Incorporated. (2012). Mineral insulated signal transmission cable [Online image]. Retrieved May 10, 2013 from http://www.thermocoax-nuclear.com/nuclear---transmission-cable-application.html.

Thermocoax Incorporated. (2012b).Thermocoax mineral insulated signal transmission cables. Retrieved January 21, 2014 from http://www.thermocoax.com/signal-transmission.html.

Tkgd2007. (2008). A cutaway diagram of a coaxial cable [Online image]. Retrieved May 26, 2013 from http://en.wikipedia.org/wiki/File:Coaxial_cable_ cutaway.svg

United States Environmental Protection Agency. (2010, November). Geologic CO_2 sequestration technology and cost analysis (Report No. 816-B-08-009). Retrieved from http://water.epa.gov/type/groundwater/uic/class6/upload/ geologicco2sequestrationtechnologyandcostanalysisnov2010.pdf

Wei, T., Wu, S., Huang, J., Xiao, H., & Fan, J. (2011). Coaxial cable Bragg grating. *Applied Physics Letters, 99*(11), 113517-113517.

Weideman, B. & Nygaard, R. (2014, April). How cement operations affect your cement sheath short and long term integrity. In *American Association of Drilling Engineers Fluids Technical Conference and Exhibition*.

Williams, G. R., Brown, G., Hawthorne, W., Hartog, A. H., & Waite, P. C. (2000, December). Distributed temperature sensing (DTS) to characterize the performance of producing oil wells. In *Environmental and Industrial Sensing* (pp. 39-54). International Society for Optics and Photonics.

Wright, I. W., Ringrose, P. S., Mathieson, A. S., & Eiken, O. (2009, January 1). An overview of active large-scale CO_2 storage projects. Society of Petroleum Engineers. doi:10.2118/127096-MS.

Wu, S., Wei, T., Huang, J., Xiao, H., & Fan, J. (2012, April). A study on Q-factor of CCBG sensors by coupled mode theory. In *SPIE Smart Structures and Materials+ Nondestructive Evaluation and Health Monitoring* (pp. 834549-834549). International Society for Optics and Photonics.

Zeidouni, M. (2014). Analytical model of well leakage pressure perturbations in a closed aquifer system. Advances in Water Resources.

Zimmer, M., Pilz, P., & Erzinger, J. (2011). Long-term surface carbon dioxide flux monitoring at the Ketzin carbon dioxide storage test site. *Environmental Geosciences, 18*(2), 119-130.

VITA

Yurong Li was born in 1990 in China. She went to high school in China and graduated in 2008. She received her Petroleum Engineering Bachelor's degree from China University of Petroleum (Huadong) in 2012, and started her Master's degree in Petroleum Engineering at Missouri University of Science and Technology. During her Master's study, she worked with Dr. Runar Nygaard as a graduate research assistant and got involved in a DOE project. She earned her Master's degree in May of 2014.